Differentiating Epileptic from Psychogenic Nonepileptic EEG Signals using Time Frequency and Information Theoretic Measures of Connectivity

Sarah Barnes

A Thesis Submitted to the Graduate Faculty of

GRAND VALLEY STATE UNIVERSITY

In

Partial Fulfillment of the Requirements

For the Degree of

Master of Science in Engineering, Biomedical Engineering

Padnos College of Engineering and Computing

December 2019

Abstract

Differentiating psychogenic nonepileptic seizures from epileptic seizures is a difficult task that requires timely recording of psychogenic events using video electroencephalography (EEG). Interpretation of video EEG to distinguish epileptic features from signal artifacts is error prone and can lead to misdiagnosis of psychogenic seizures as epileptic seizures resulting in undue stress and ineffective treatment with antiepileptic drugs. In this study, an automated surface EEG analysis was implemented to investigate differences between patients classified as having psychogenic or epileptic seizures. Surface EEG signals were grouped corresponding to the anatomical lobes of the brain (frontal, parietal, temporal, and occipital) and central coronal plane of the skull. To determine if differences were present between psychogenic and epileptic groups, magnitude squared coherence (MSC) and cross approximate entropy (C-ApEn) were used as measures of neural connectivity. MSC was computed within each neural frequency band (delta: 0.5Hz-4Hz, theta: 4-8Hz, alpha: 8-13Hz, beta: 13-30Hz, and gamma: 30-100Hz) between all brain regions. C-ApEn was computed bidirectionally between all brain regions. Independent samples t-tests were used to compare groups. The statistical analysis revealed significant differences between psychogenic and epileptic groups for both connectivity measures with the psychogenic group showing higher average connectivity. Average MSC was found to be lower for the epileptic group between the frontal/central, parietal/central, and temporal/occipital regions in the delta band and between the temporal/occipital regions in the theta band. Average C-ApEn was found to be greater for the epileptic group between the frontal/parietal, parietal/frontal, parietal/occipital, and parietal/central region pairs. These results suggest that differences in neural connectivity exist between psychogenic and epileptic patient groups.

Table of Contents

List of Tables

List of Figures

Abbreviations

EEG-Electroencephalogram

ES-Epileptic Seizure (also referred to as “neurogenic”)

PNES-Psychogenic Nonepileptic Seizure

MSC-Magnitude Squared Coherence

C-ApEn-Cross Approximate Entropy

AED-Antiepileptic Drug

Chapter 1. Introduction

1.1 Introduction

A seizure is an abrupt event which affects at least one of the sensory, motor, or autonomic functions [1]. Seizures can be broadly categorized into two groups: “neurogenic” or epileptic seizures (ES) and “psychogenic” nonepileptic seizures (PNES). Clinical presentation of ES and PNES are often similar, affecting the sensory, motor, autonomic, and/or psychic functions and can include impairment or loss of consciousness, involuntary movements, and alterations in behavior [1], [2]. The primary distinguishing characteristic is abnormal neural activity, which is present during ES but not during PNES, suggesting that PNES are not neurological in origin [1]-[3]. The focus of this study is on differentiating between two groups of patients: those who experience ES and those who experience PNES. Surface electroencephalogram (EEG) is a recording technique that measures the brain’s electrical activity via surface electrodes placed on the scalp. EEG recordings capturing various neural states including, normal wakefulness, sleep, psychogenic, and epileptic events, from the two groups will be evaluated for differences in neural activity.

Confusion of the symptoms of ES and PNES can result in diagnostic delays of 7-10 years [4]. PNES are often classified as ES leading to patients being treated with antiepileptic drugs (AEDs). The use of AEDs to treat PNES has been shown to be ineffective and may actually result in worsening of symptoms [2]-[5]. Currently, video EEG is the gold standard for the diagnosis of PNES [5]. Video EEG combines surface EEG and video recording to allow clinicians to observe the physical presentation of a seizure while measuring electrical neural activity to identify the epileptic discharges that are indicative of an ES. This has been deemed the most effective and accurate form of diagnosis for PNES [2]. However, video EEG requires

recording while the patient is having an active seizure making it best suited for patients who experience frequent seizures. Additionally, video EEG is time consuming and may cause the patient unwanted stress due to anticipation of a seizure and desire to replicate symptoms [2].

Automated EEG analysis can be used to aide in the detection of abnormal brain activity and, more importantly, to potentially discriminate between neurogenic and psychogenic seizures. While EEG signals have been analyzed using nonparametric time-frequency and information theoretic measures to predict, detect, and classify seizure events in epileptic patients [6]–[14], few studies have directly applied these techniques to differentiate PNES from ES. Outside of EEG analysis, MRI based studies have shown that epilepsies are associated with brain network abnormalities, yet few of these studies have been applied to study PNES [4].

Magnitude squared coherence (MSC) and cross approximate entropy (C-ApEn) are nonparametric time-frequency and information theoretic measures, respectively. Both are measures of the statistical similarity between two time series in a network. MSC measures how well two time series match one another at various frequencies [13]. C-ApEn measures the pattern complexity of two interconnected time series [15], [16]. In this study MSC and C-ApEn were applied to surface EEG data to provide a measure of how the regions of the brain interact in patients who experience neurogenic seizures versus patients who experience psychogenic seizures. Furthermore, MSC allowed for evaluation of brain region interactions within the brain wave frequency bands.

1.2 Purpose

The purpose of this study was to explore differences in neural connectivity in surface EEG recordings from patients who experience ES versus patient who experience PNES. Due to the underlying differences between the seizure types, it was expected that the two patient groups would exhibit neural differences during both normal and seizure activity as recorded using surface EEG. MSC and C-ApEn were used to perform connectivity measures between brain regions to obtain a better understanding of how various regions of the brain interact. The goal was to identify differences in connectivity between the two patient groups that could act as a biomarker using surface EEG recordings alone. A successful biomarker could be implemented as a means for seizure type classification and would be valuable to clinicians during the epileptic diagnostic process.

1.3 Scope

The focus of this study was on how regions of the brain interact in patients who suffer from ES or PNES through analysis of surface EEG recordings. MSC was used as a time-frequency measure of linearity in phase relationship between two surface EEG signals. C-ApEn was used as a nonlinear information theoretic measure of complexity between two surface EEG signals. Deidentified EEG signal data were provided by the Spectrum Health Office of Clinical Research in conjunction with the Epilepsy Monitoring Unit. Data were recorded using the standard clinical 10-20 surface EEG system. Channel electrode signals were selected according to the 10-20 protocol and combined to represent regions corresponding to the anatomical features of the brain. Five regions of interest were identified: (1) Frontal, (2) Parietal, (3) Temporal, (4) Occipital, and (5) Central. The first four regions correspond to electrode placement over the four lobes of the

brain, while the fifth region corresponds to the central recording electrodes placed along the coronal plane. Using the provided surface EEG data, MSC and C-ApEn were computed between all regions of the brain over all time and for all subjects. Differences in region-region interactions between the epileptic and nonepileptic groups were evaluated for statistical importance. Mean MSC in the region-region interactions were further evaluated in the brain wave frequency bands: (1) Delta (0.5-4Hz), (2) Theta(4-8Hz), (3) Alpha(8-13Hz), (4) Beta(13-30Hz), and (5) Gamma(30-100Hz), to identify differences in neural activity between the two patient groups.

1.4 Assumptions

For this study, it was assumed that each patient had been accurately classified as suffering from ES or PNES. The assumption of independence between ES and PNES allowed for comparison between the two groups. It was expected that some of the data contained physiological artifact due to movement and hyperventilation based on EEG interpretations for each patient provided by Spectrum Health. Additionally, it was assumed that surface EEG recordings were not necessarily taken during active seizure events. This assumption was based from the patient notes prepared by the neurologist indicating normal wakefulness, sleep, and seizure activity throughout the length of the recordings. The time of occurrence of events were not indicated in the patient notes, therefore it was assumed that the surface EEG data were representative of a mixture of both normal signals and non-normal (psychogenic or epileptiform) signals.

1.5 Hypothesis

Previous studies have found that epilepsies have been associated with brain network abnormalities [4]. Of the few studies that have investigated PNES, findings suggest that PNES may be correlated with altered interactions between brain areas suggesting that network information could be a potential indicator for PNES differentiation [4]. In comparing ES and PNES groups, studies have found that patients classified as experiencing ES or PNES have different brain connectivity than individuals who do not experience seizures, but patients exhibiting psychogenic type seizures were not as easily distinguished from those exhibiting neurogenic type using connectivity measures [4]. These findings suggest a need for a more robust way to differentiate between ES and PNES. Some techniques that have been applied in seizure detection and classification include exploration of differences in lobal connectivity [4], [6], [7], entropies [8], [9], and time frequency analysis [7], [11]. Theoretically, surface EEG signals recorded during ES or PNES should be distinctive due to the differences in the physiological nature of the two types of seizures. Because ES and PNES were expected to exhibit differences in neural activity, time frequency and entropy analysis were implemented to determine if differences could be identified from surface EEG recordings. For this study, the available surface EEG data analyzed included various states of neural cognizance including normal wakefulness, sleep, and possible seizure activity. It was hypothesized that the application of time-frequency and information theoretic measures would reveal differences in neural connectivity with respect to brain region interactions and neural frequency band as measured using MSC and C-ApEn.

1.6 Significance

The primary goal of this study was to provide Spectrum Health with information to aid in the differentiation of epileptic from psychogenic nonepileptic seizures during the diagnosis phase. The application of MSC and C-ApEn to surface EEG recordings between brain regions and within the neural frequency bands was implemented to increase understanding of differences in neural connectivity between psychogenic and neurogenic groups and to identify a potential biomarker. The current process for classifying patients as experiencing ES or PNES has proved to be lengthy and difficult one. A well-defined biomarker could provide value to clinicians in automating the process of seizure type analysis to increase diagnostic and workload efficiencies.

1.7 Definitions

Epileptic Seizure: A seizure that involves irregular neuronal activity in the brain.

Psychogenic Nonepileptic Seizure: An event that resembles the physical and sensational aspects of an epileptic seizure but lacks irregular neuronal activity in the brain.

Magnitude Squared Coherence: A frequency measure that estimates the similarity of two time series.

Cross Approximate Entropy: A measure of the conditional complexity of two time series.

Chapter 2. Differentiating Epileptic from Psychogenic Nonepileptic EEG Signals using Time Frequency and Information Theoretic Measures of Connectivity

Abstract

Differentiating psychogenic nonepileptic seizures from epileptic seizures is a difficult task that requires timely recording of psychogenic events using video electroencephalography (EEG). Interpretation of video EEG to distinguish epileptic features from signal artifacts is error prone and can lead to misdiagnosis of psychogenic seizures as epileptic seizures resulting in undue stress and ineffective treatment with antiepileptic drugs. In this study, an automated surface EEG analysis was implemented to investigate differences between patients classified as having psychogenic or epileptic seizures. Surface EEG signals were grouped corresponding to the anatomical lobes of the brain (frontal, parietal, temporal, and occipital) and central coronal plane of the skull. To determine if differences were present between psychogenic and epileptic groups, magnitude squared coherence (MSC) and cross approximate entropy (C-ApEn) were used as measures of neural connectivity. MSC was computed within each neural frequency band (delta: 0.5Hz-4Hz, theta: 4-8Hz, alpha: 8-13Hz, beta: 13-30Hz, and gamma: 30-100Hz) between all brain regions. C-ApEn was computed bidirectionally between all brain regions. Independent samples t-tests were used to compare groups. The statistical analysis revealed significant differences between psychogenic and epileptic groups for both connectivity measures with the psychogenic group showing higher average connectivity. Average MSC was found to be lower for the epileptic group between the frontal/central, parietal/central, and temporal/occipital regions in the delta band and between the temporal/occipital regions in the theta band. Average C-ApEn was found to be greater for the epileptic group between the frontal/parietal,

parietal/frontal, parietal/occipital, and parietal/central region pairs. These results suggest that differences in neural connectivity exist between psychogenic and epileptic patient groups.

2.1 Introduction

Seizures are involuntary and abrupt events which affect at least one of the sensory, motor, or autonomic functions [1]. Epileptic seizures (ES) and psychogenic nonepileptic seizures (PNES) share many of the characteristic movements, sensations, and experiences that occur during a seizure but differ in their underlying etiology. ES or "neurogenic" seizures stem from an underlying neurological condition and are marked by epileptic discharges resulting from abnormal and/or synchronous brain activity [17]. In contrast, these epileptic discharges are absent during PNES. As the term "psychogenic" implies, PNES are psychological in origin and have been diagnostically classified as dissociative or somatoform disorders and are thought to be a stress response that can be physical, emotional, or social in nature [1]-[3], [5], [10].

The closeness in physical presentation can make differentiating between ES and PNES particularly challenging. The current process of psychogenic seizure classification relies heavily on careful evaluation of video electroencephalography (EEG) by an experienced physician during an active seizure event. This real-time requirement makes video EEG unsuitable for patients whose seizure events are infrequent and unpredictable. A high level of expertise is required to accurately identify epileptic discharges in EEG signals from artifacts arising from movements, breathing, and environmental noise that can have similar signal appearance. This strict process of distinguishing between psychogenic and neurogenic seizures can result in diagnostic delays as great as 7-10 years [4], suggesting a need for additional methods that could be applied to increase efficiency and accuracy.

Automated signal processing is complimentary to complex bio-signals like those of the human brain [6]-[14]. More specifically, automated EEG analysis can be used to aide in the detection of abnormal brain activity and, more importantly, to potentially discriminate between neurogenic and psychogenic seizures. EEG signals have been analyzed to predict, detect, and classify seizure events in epileptic patients through exploration of differences in lobal connectivity [4], [6], [7], entropies [8], [9], and time frequency analysis [7], [11]. However, few of these techniques have been directly applied to evaluate differences between epileptic and psychogenic groups.

Previous studies have found that epilepsies have been associated with brain network abnormalities [4]. Of the few studies that have investigated PNES, findings suggest that PNES may be correlated with altered interactions between brain areas suggesting that network information could be a potential indicator for PNES differentiation [4]. In comparing ES and PNES groups, studies have found that patients classified as experiencing ES or PNES have different brain connectivity than individuals who do not experience seizures, but patients exhibiting psychogenic type seizures are not as easily distinguished from those exhibiting neurogenic type seizures using connectivity measures [4].

In theory surface EEG signals recorded from patients who experience ES and PNES should be distinctive due to the differences in their physiological nature. In this study magnitude squared coherence (MSC) and cross approximate entropy (C-ApEn) will be used to evaluate neural connectivity between brain regions during both normal activity and seizure activity as recorded using surface EEG obtained from two sets of patients: those who experience neurogenic seizures and those who experience psychogenic seizures. The time-frequency feature of MSC will be used to further investigate brain region interactions in the delta (0.5-4Hz), theta(4-8Hz),

alpha(8-13Hz), beta(13-30Hz), and gamma(30-100Hz) frequency bands. These techniques will increase understanding of how various regions of the brain interact while revealing any differences in neural connectivity in the two patient groups that could be implemented during the process of epileptic and psychogenic seizure type distinction.

2.1 Methods

2.2.1 Subject Data

Deidentified surface EEG recordings from 18 subjects were provided to Grand Valley State University by the Spectrum Health Office of Clinical Research in conjunction with the Epilepsy Monitoring Unit. Subjects were categorized into two groups based on the incidence of psychogenic or epileptic seizures: 0 (control or psychogenic) or 1 (epileptic). EEG signals were recorded using the international standard 10-20 protocol. The surface EEG recordings for all patients had a sampling rate of 200 Hz. Length of recording varied from 8.7 minutes to 10.5 minutes. Subject numbers, grouping, and EEG interpretations were provided along with the EEG data. EEG interpretation notes gave limited information about the subject's state during recording (sleep or wakefulness), the presence of seizure activity (psychogenic or epileptic) and artifacts, as well as the suspected type of epilepsy for subjects in the epileptic group. The timing of events was not specified in the patient notes. The EEG interpretations indicated that the surface EEG data provided from all subjects were therefore representative of a combination of both normal EEG signals and non-normal (psychogenic or epileptiform) EEG signals. See Appendix A for EEG interpretation notes.

2.2.2 Data Analysis

All surface EEG signals were analyzed using non-parametric information theoretic and time-frequency measures to assess network connectivity between regions of the brain using MATLAB R2019a. Five brain regions were selected for analysis: (1) Frontal, (2) Parietal, (3) Temporal, and (4) Occipital corresponding to the lobes of the brain, as well as a (5) Central region that corresponds to the positional placement of recording electrodes along the coronal plane. Figure 2.1 demonstrates the placement of electrodes according to the 10-20 standard with the brain regions labeled.

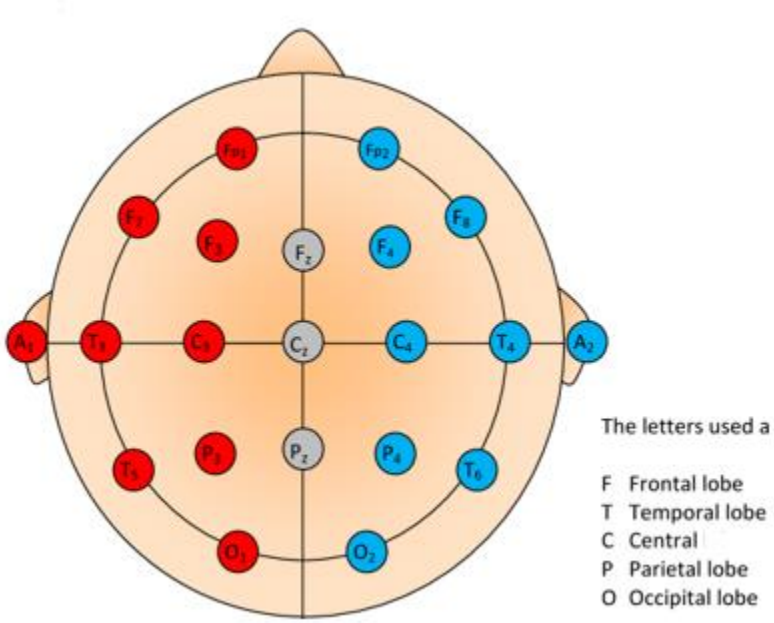

Figure 2.1. Electrode placement for EEG recording with brain region labels [18]

A total of 10 pairs of regions were evaluated. Regions were not split by anatomical hemisphere. The region pairs are shown in Table 2.1.

Table 2.1. Region Pairs of Interest

Region Number	Region Pair
1	Frontal / Parietal
2	Frontal / Temporal
3	Frontal / Occipital
4	Frontal / Central
5	Parietal / Temporal
6	Parietal / Occipital
7	Parietal / Central
8	Temporal / Occipital
9	Temporal / Central
10	Occipital / Central

Frequency analysis further allowed for evaluation of connectivity between brain regions in the neural frequency bands: Delta (0.5-4 Hz), Theta (4-8 Hz), Alpha (8-13 Hz), Beta(13-30 Hz), and Gamma (30-100 Hz). The diagram in Figure 2.2 illustrates the full data analysis process.

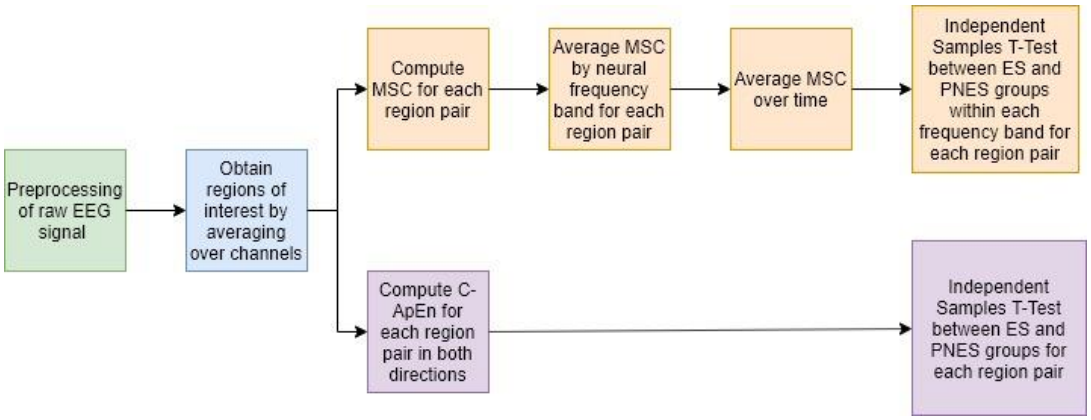

Figure 2.2. Functional block diagram of the data analysis process

2.2.2.1 Preprocessing

A 2nd order Butterworth notch filter at 60 Hz was applied to the raw surface EEG signals to remove powerline interference. A reference average was applied by subtracting the average of all the EEG electrodes from the EEG signal for all subject data.

2.2.2.2 Brain Regions of Interest

The surface EEG data consisted of 23 recording channels based on the international standard 10-20 protocol for EEG electrode placement. EEG signal channels were extracted and grouped according to Table 2.2. The EEG signals were averaged within each group to obtain a single representative time series for each brain region.

Table 2.2. EEG Signal Channels Grouping for each Brain Region

Brain Region	**EEG Signal Channels**					
Frontal	'Fp1'	'Fp2'	'F3'	'F4'	'F7'	'F8'
Parietal		'P3'	'P4'	'P7'	'P8'	
Temporal		'T7'	'T8'	'T1'	'T2'	
Occipital			'O1'	'O2'		
Central			'C3'	'C4'		

2.2.2.3 Magnitude Squared Coherence

Magnitude squared coherence (MSC) is a technique that measures the linear relationship between two time series as a function of frequency and is defined by

$$MSC(n,k) = \frac{|S_{xy}(n,k)|^2}{S_{xx}(n,k)S_{yy}(n,k)} \qquad (2.1)$$

where Sxx and Syy are the auto power spectra and Sxy is the cross power spectrum of the input signals $x(n)$ and $y(n)$, n is the time index, and k is the frequency index. The approach used for calculating MSC was proposed by Lovett and Ropella [19]. To begin, the short term minimum bias eigentransform (STET) was computed for the input signals to obtain $X_l[n,k]$ and $Y_l[n,k]$ defined by

$$X_l[n,k] = \sum_{m=0}^{M-1} x\left[n+m-\frac{M}{2}\right] V_l[m] e^{-j2\pi mk/M} \qquad (2.2)$$

where $x[n-m-M/2]$ is a the input signal to be evaluated at n time points with percent overlap of $M/2$, $V_l[m]$ is spheroidal sequence of l mutli-taper windows of length M, and k is the frequency index. Using the results of the STET, the power spectra were computed as

$$S_{xx} = |\sum_{l=0}^{L-1} X_l[n,k]|^2 \qquad (2.3)$$

$$S_{yy} = |\sum_{l=0}^{L-1} Y_l[n,k]|^2 \qquad (2.4)$$

$$S_{xy} = \sum_{l=0}^{L-1} X_l[n,k] Y_l^*[n,k] \qquad (2.5)$$

MSC values lie between 0 and 1, revealing the linearity of phase relationship of two signals over time [19]. An MSC value of 0 indicates a zero linear relationship while an MSC value of 1 indicates an ideal linear relationship.

An algorithm to compute $MSC(n,k)$ was developed in MATLAB R2019a to evaluate neural connectivity between brain regions in the neural frequency bands. A spheroidal sequence of L = 7 mutli-taper windows with M = 1200 was generated using MATLAB's discrete prolate spheroidal (Slepian) sequences (DPSS) function. Since fs = 200 Hz, the window length, M, was chosen to achieve a time resolution of 6 seconds and a frequency resolution of 0.167 Hz. The number of FFT points were chosen as 1200 to match the window length. The time increment was set to 600 for 50% overlap.

For all subjects, coherence spectrograms were obtained for each region pair spanning the neural frequency bands for the full length of recording. The region pair MSC values were further manipulated to obtain average MSC time series for each of the neural frequency bands. Finally, the time series data were averaged once more to obtain a single coherence value for each region in each neural frequency band. Figure 2.3 illustrates the process that was taken to obtain the final MSC averages.

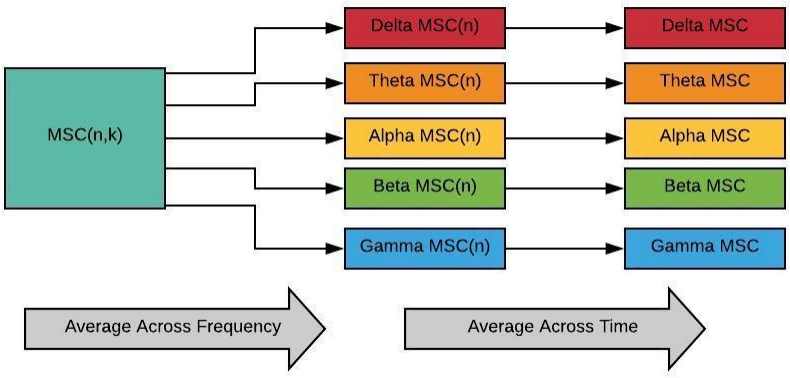

Figure 2.3. Flow Diagram of MSC Average Calculations

2.2.2.4 Cross Approximate Entropy

Cross approximate entropy ($C - ApEn$) is a non-linear directed measure that describes the pattern complexity or similarity between two times series $x(n)$ and $y(n)$, defined by

$$C - ApEn(m, r, N) = \Phi_{xy}^{m}(r) - \Phi_{xy}^{m+1}(r) \qquad (2.6)$$

where m is the dimension that describes the length of each data block to be compared, r is a threshold that acts as a noise filter, and N is the total length of the data. The process for computing C-ApEn is as follows: For two times series, $x(n)$ and $y(n)$, the length dimension m and the threshold r are selected. As suggested by the literature [20], the value of m is usually chosen as 2 and the value of r is taken as $0.2SDx$ where SDx is the standard deviation of the data $x(n)$ The input signals, $x(n)$ and $y(n)$, are normalized by subtracting the average of the signal and dividing by the standard deviation so that $SDx = SDy = 1$.

$$x'(n) = \frac{x(n) - \overline{x(n)}}{SDx} \qquad (2.7)$$

$$y'(n) = \frac{y(n) - \overline{y(n)}}{SDy} \qquad (2.8)$$

Two sets of vectors X(i) and Y(j) of length m are created:

$$X(i) = [x(i), x(i+1), \dots, x(i+m-1), \quad i = 1, N-m+1 \qquad (2.9)$$

$$Y(j) = [y(j), y(j+1), \dots, y(j+m-1), \quad j = 1, N-m+1 \qquad (2.10)$$

The distance between vectors is defined as the absolute maximum difference between X(i) and Y(j):

$$d[X(i)\ Y(j)] = max_{k=0,m-1}[|x(i+k) - y(j+k)|] \qquad (2.11)$$

For a given X(i), the number of distances, $\mathrm{d[X(i)\ Y(j)]}, (\mathrm{j} = 1, \mathrm{N} - \mathrm{m} + 1)$ that are close to the m-point pattern formed by $X(i)$ within the threshold tolerance of $\pm r$ are found:

$$N_{xy}^{m}(i) = \#\ of\ d[X(i)\ Y(j)] \leq r \qquad (2.12)$$

The ratio of $\mathrm{N_{xy}^{m}(i)}$ to the total number of all m-point patterns, $(\mathrm{N} - \mathrm{m} + 1)$ is then calculated to determine the frequency of occurrence of the m-point y patterns formed by Y(j), $(\mathrm{j} = 1, \mathrm{N} - \mathrm{m} + 1)$, being within the threshold tolerance of $\pm \mathrm{r}$ to the m-point x pattern of a given X(i):

$$C_{xy}^{m}(i) = \frac{N_{xy}^{m}(i)}{N-m+1} \qquad (2.13)$$

Computation of $\mathrm{N_{xy}^{m}(i)}$ and $C_{xy}^{m}(i)$ is repeated for all $X(i), (i = 1, N - m + 1)$. Next, the average frequency that all m-point patterns in $Y(j)$ remain close for all m-point patterns in $X(i)$, $\Phi_{xy}^{m}(r)$, is found by taking the natural logarithm of the ratio, $\mathrm{C_{xy}^{m}(i)}$ and averaging over i.

$$\Phi_{xy}^{m}(r) = \frac{1}{N-m+1}\sum_{i=1}^{N-m+1} \ln C_{xy}^{m}(i) \qquad (2.14)$$

The previous steps are repeated for $\mathrm{m}+1$ to obtain $\Phi_{\mathrm{xy}}^{\mathrm{m}+1}(\mathrm{r})$. Finally, $\mathrm{C}-\mathrm{ApEn}(\mathrm{m},\mathrm{r},\mathrm{N})$ is found using Eqn. 2.6.

For $m = 2$, the meaning of $C - ApEn(m, r, N)$ can be interpreted as the difference between the average frequency that all 2-point patterns in $Y(j)$ remain close for all 2-point patterns in $X(i)$ and the average frequency that all 3-point patterns in $Y(j)$ remain close for all 3-point patterns in $X(i)$. Intuitively, this provides the rate of new pattern generation from dimension $m = 3$ to $m = 2$ and thus the cross complexity of the two time series signals $x(n)$ and $y(n)$ [26]. A larger value of $C - ApEn$ would indicate higher complexity between the two signals and thus lower connectivity. Because $C - ApEn$ is a directed measure, it also provides a way to assess how connectivity varies based on directionality. In other words, $C - ApEn$ is different from $x(n)$ to $y(n)$ as compared to $y(n)$ to $x(n)$. This allows for the establishment of not only connectivity but also directionality.

A $C - ApEn$ algorithm was developed in MATLAB 2019a to evaluate neural connectivity between brain regions. The dimension m defines the length of the data segments to be compared and was chosen as 2 and the threshold r was chosen as $0.2SD$, where SD represents the standard deviation of the input signals $x(n)$ and $y(n)$. Each time series was normalized to obtain a $SD = 1$. Region pairs were evaluated in both directions, i.e. $C - ApEn$ was computed for 20 cases per subject.

An additional time entropy analysis was implemented to observe how $C - ApEn$ changed over time for EEG signals recorded from an ES subject and a PNES subject. Subjects were selected based on the indication of a seizure event according to the EEG interpretation notes. $C - ApEn$ was computed between the parietal/central brain region pair in the parietal to central direction at 5

second (1200 pt.) time intervals for one subject from each group. The $C - ApEn$ values were plotted to investigate changes in $C - ApEn$ over time.

2.2.3 Statistical Analysis

An independent samples t-test was performed between epileptic and psychogenic groups for each region pair in each frequency band of interest for MSC and for each region pair (bi-directionally) for C-ApEn. This method of statistical analysis was implemented to determine if there was an overall difference in neural connectivity between the two patient groups as measured by MSC and C-ApEn. The epileptic and psychogenic groups were assumed to be independent groups with independence of observations. Equal variances were not assumed. Normality and outliers were assessed using the descriptive statistics toolset in SPSS. The Shapiro-Wilk test was used to check for normality and boxplots were used to determine the presence of outliers within groups. Due to the variability in patient state during recording as noted in the EEG interpretations (Appendix A), outliers were expected to be present and therefore not removed from the initial analysis of MSC and C-ApEn. For C-ApEn, outliers appearing consistently were removed from the analysis and independent samples t-tests were repeated.

2.3 Results

2.3.1 Raw EEG Signals

Raw EEG data from one subject in the epileptic group and one subject in the psychogenic group were plotted in MATLAB for visual comparison. Raw signals from a frontal lead, parietal lead, and occipital lead are shown for 350 seconds of recording in Figure 2.4. Differences in the

raw EEG signals from each signal lead between the two groups were not obvious through visual inspection.

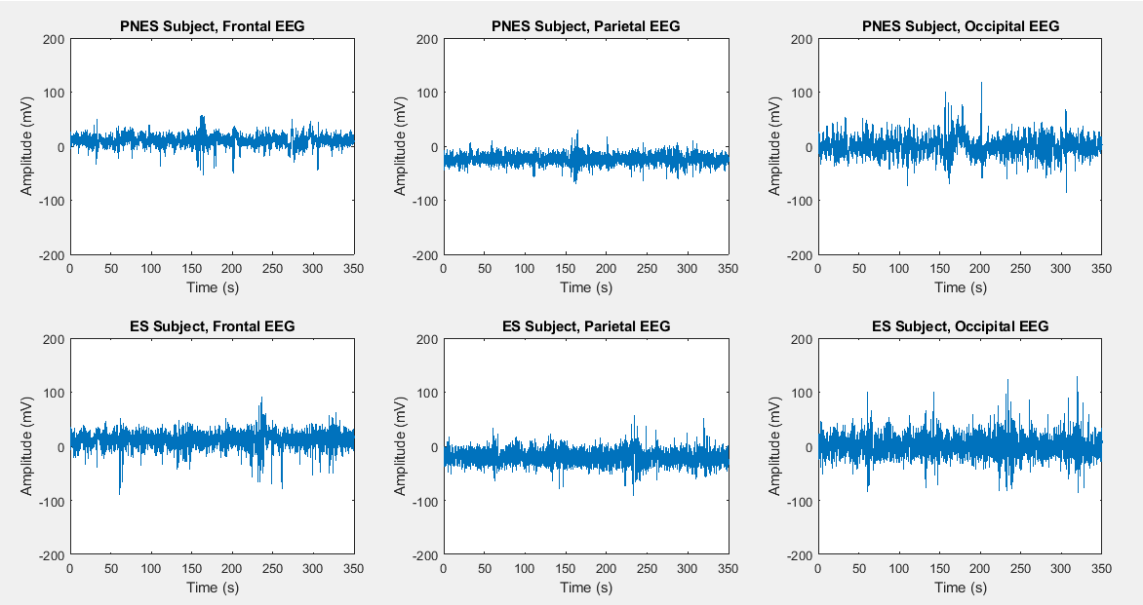

Figure 2.4. Raw EEG signals from frontal, parietal, and occipital leads from PNES and ES groups

2.3.2 Magnitude Squared Coherence

2.3.2.1 Coherence Spectrograms

MSC was computed between all regions across the full neural frequency range (0-100 Hz) to obtain coherence spectrograms. Coherence spectrograms for each region pair from one subject in each group (S8 and S15) are shown in Figure 2.5 and Figure 2.6. The spectrograms were selected to provide examples of MSC from an EEG recording where a 'psychogenic' event occurred (S8), and an EEG recording where an 'epileptic' event occurred (S15) as indicated by the EEG interpretation notes. The remaining coherence spectrograms for all subjects are shown in Appendix B – MSC Figures.

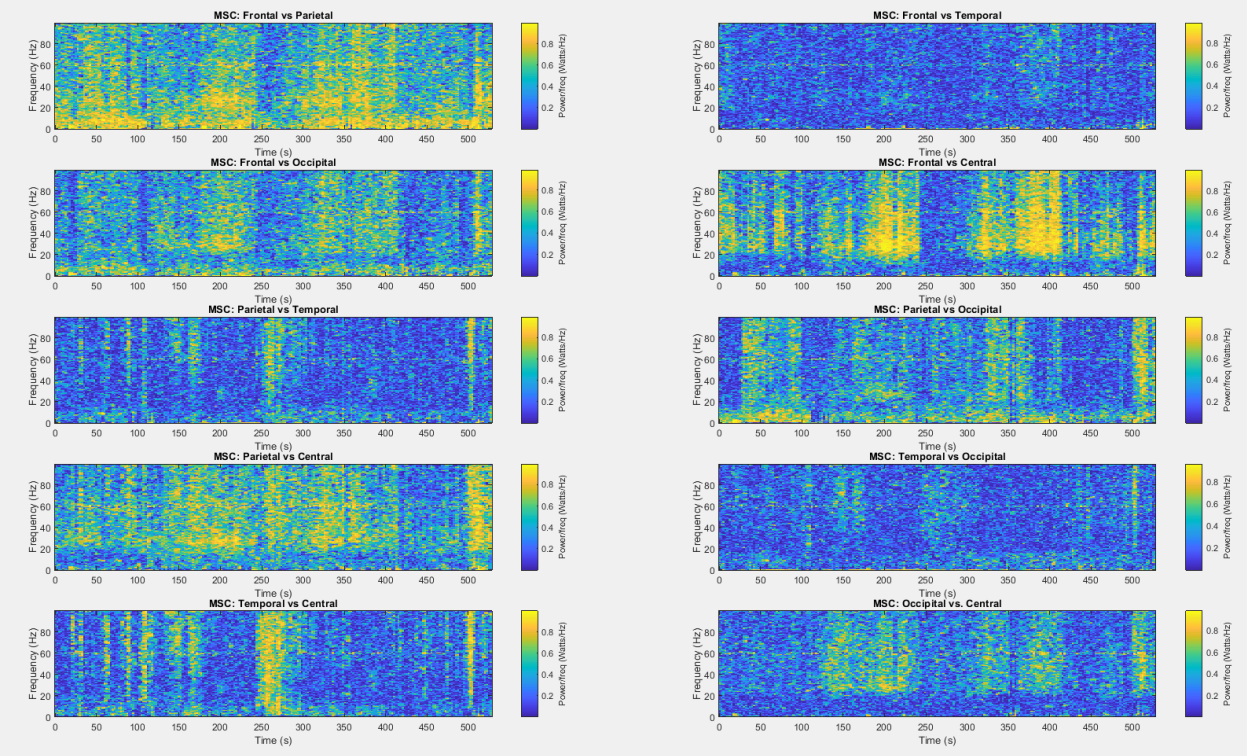

Figure 2.5. Coherence spectrogram psychogenic event: Subject 8

From Figure 2.5, coherence was low for frequencies <20Hz apart from the frontal/parietal and parietal/occipital region pairs showing some elevated coherence at lower frequencies. Coherence was low between the frontal/temporal and temporal/occipital regions across time and frequency. For the frontal/parietal, frontal/occipital, and frontal/central regions elevated coherence was observed from 0-250 seconds and 300-500 seconds with a prominent decrease in coherence from 250-300 seconds. In contrast, the opposite pattern was observed for the temporal/central region pair, which showed an increase in coherence between 250-300 seconds. Elevated coherence was also observed between the parietal/central regions.

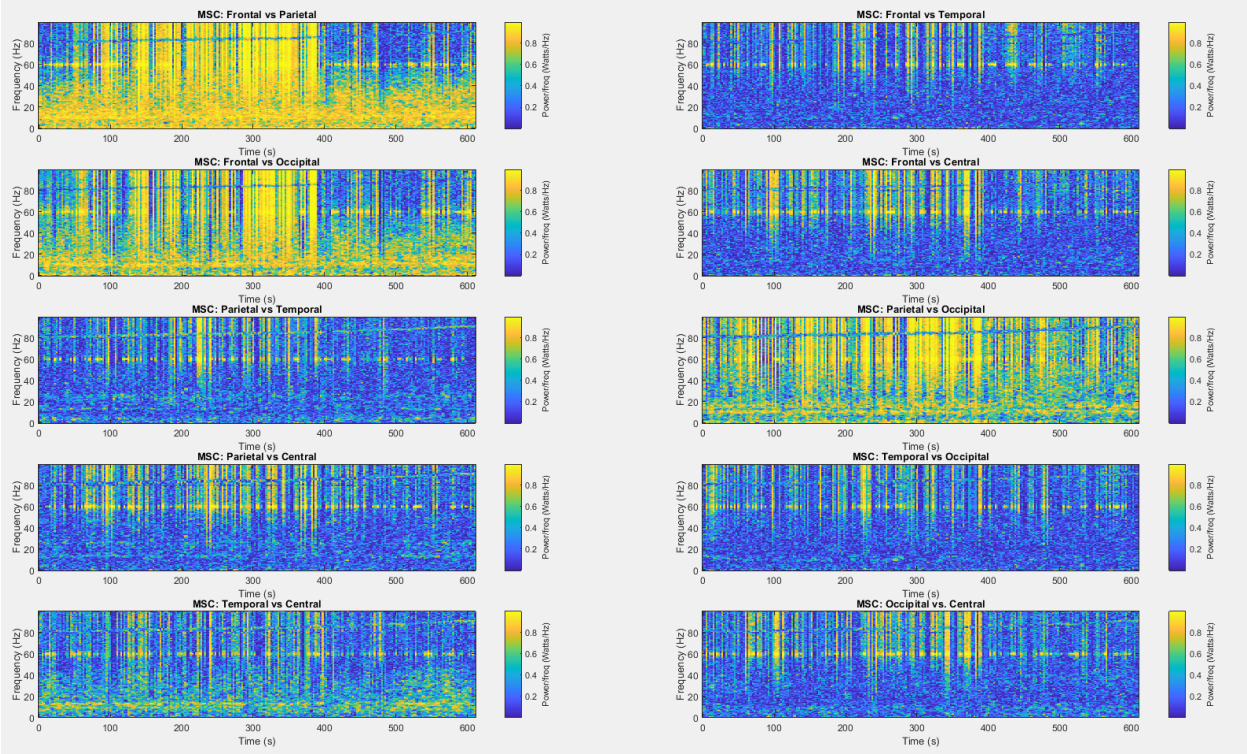

Figure 2.6. Coherence spectrogram epileptic event: Subject 15

From Figure 2.6, the coherence spectra for each region pair showed broad band increases in coherence across time with the largest increases seen between 200-400 seconds. Coherence was the highest between the frontal/parietal, frontal/occipital, and parietal/occipital regions. The remaining region pairs showed similar patterns in coherence of a lesser degree.

In comparing the two groups, coherence in the ‘ES’ spectrogram showed what appeared to be broad band spikes in coherence, from 0-100Hz, particularly in the frontal/parietal, frontal/occipital, and parietal/occipital region pairs, while coherence in the ‘PNES’ spectrogram showed increases in coherence in a more gradual manner. Both groups showed elevated coherence in the frontal/parietal, frontal/central/ parietal/occipital region pairs.

2.3.2.2 Mean MSC

The MSC spectra between each region pair were averaged over the five neural frequency band ranges and over all time for each subject (Figure 2.7 – Figure 2.11). Mean MSC for each region pair in each neural frequency band were compared using an independent samples t-test (H_o: *No differernce in MSC between ES and PNES*). A * indicates significance for p<0.10 and ** indicates significance for p<0.05. See Appendix C for data normality and outlier results.

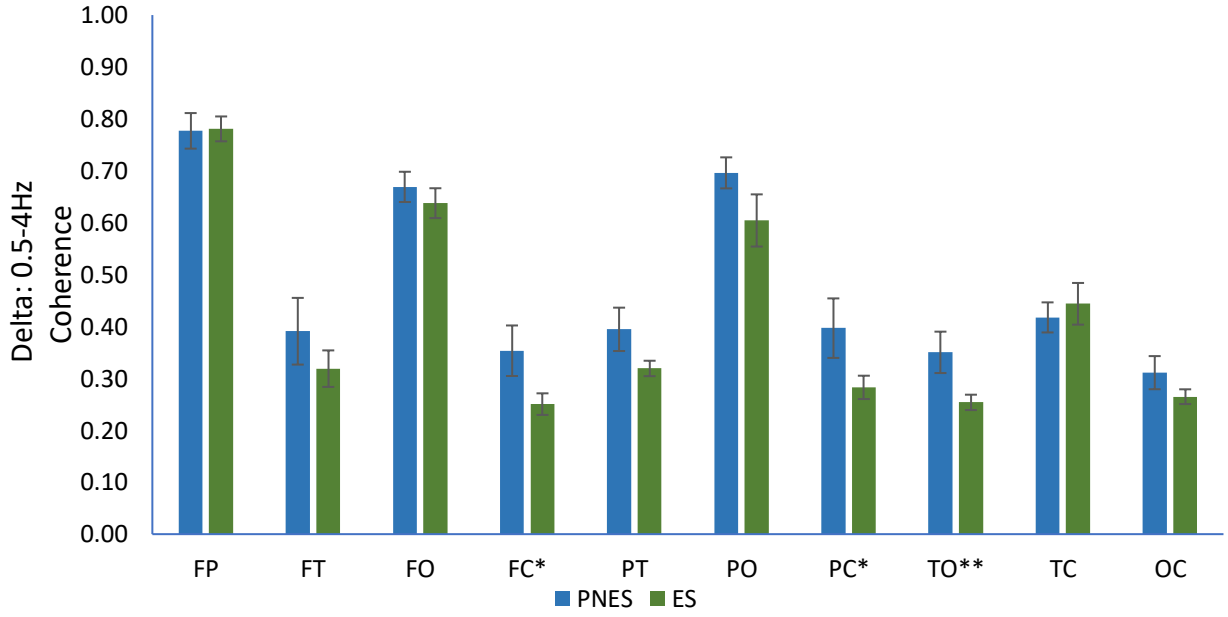

Figure 2.7. Average and standard error of the mean MSC in the Delta band

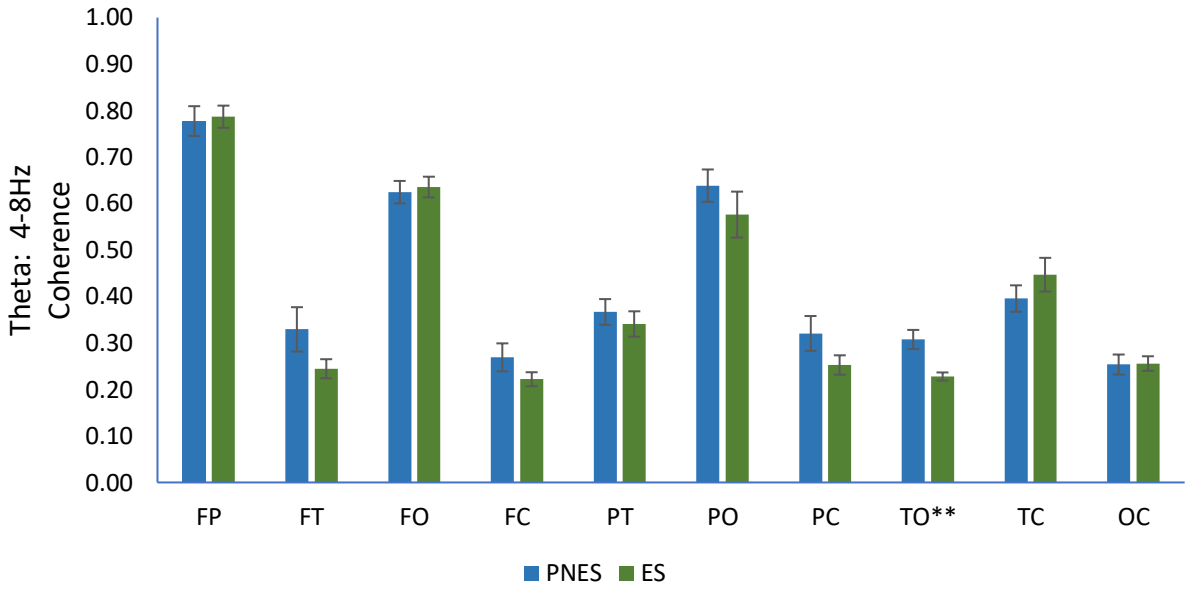

Figure 2.8. Average and standard error of the mean MSC in the Theta band

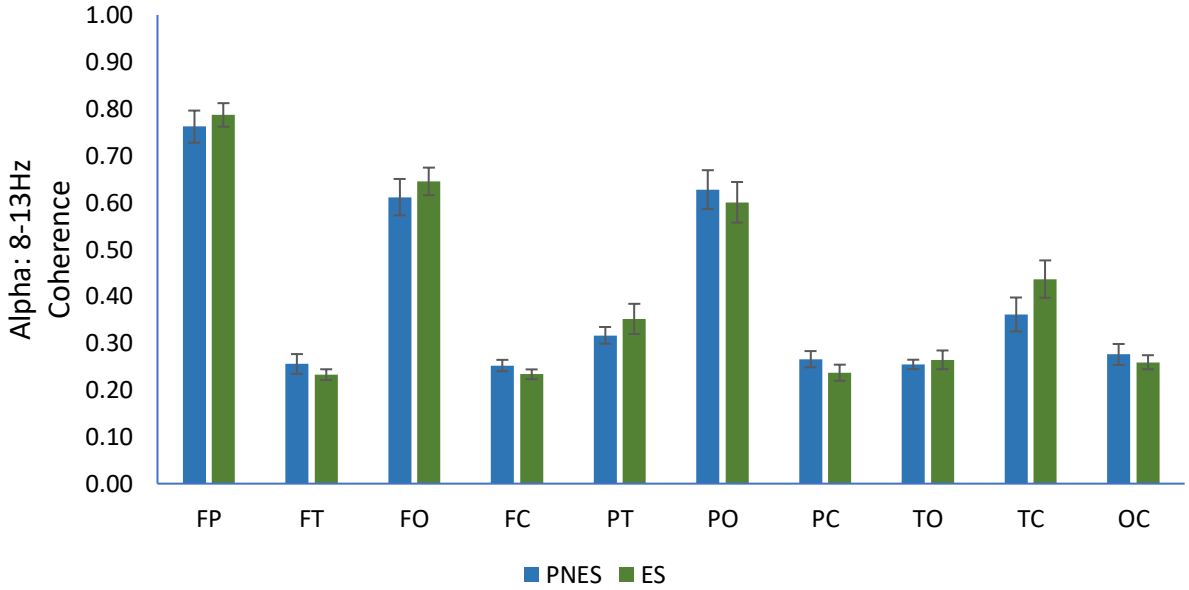

Figure 2.9. Average and standard error of the mean MSC in the Alpha band

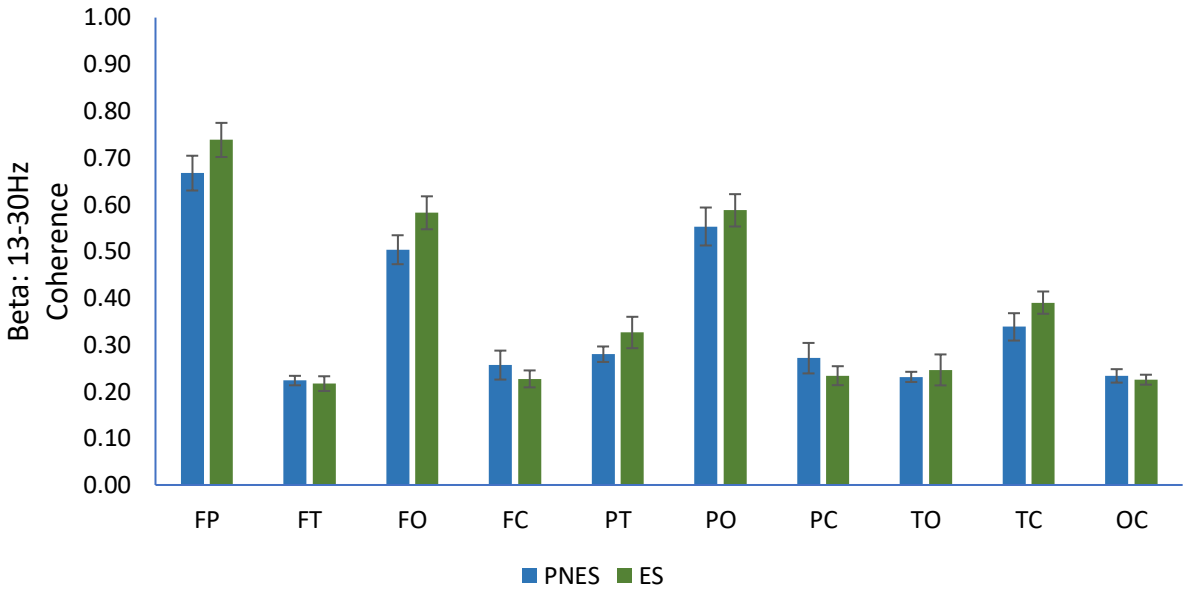

Figure 2.10. Average and standard error of the mean MSC in the Beta band

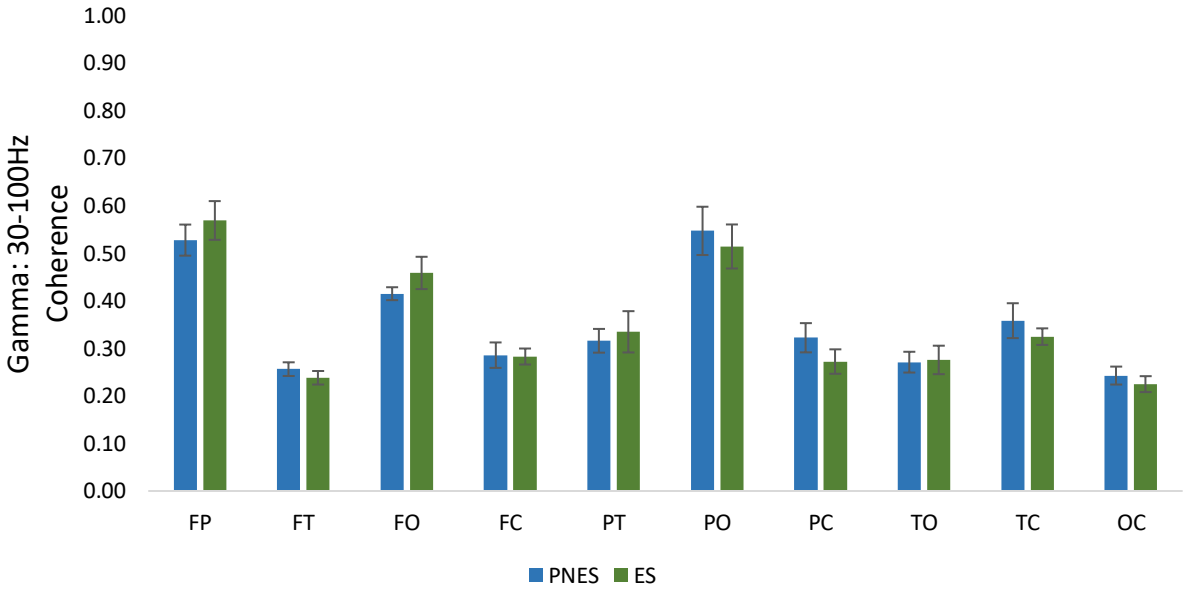

Figure 2.11. Average and standard error of the mean MSC in the Gamma band

In the delta band, (Figure 2.7), average coherence between the frontal/central regions, the parietal/central regions, and the temporal/occipital regions for the psychogenic group were found

to be significantly larger than that of the epileptic group. All other coherence differences were not significant. Based on appearance, average coherence was largest between the frontal/parietal regions for both groups. High average coherence was also observed between the frontal/occipital regions and between the parietal/occipital regions. The psychogenic group showed higher average coherence than the epileptic group for 8 out of the 10 region pairs, with the epileptic group only showing higher coherence between the frontal/parietal regions and between the temporal/central regions.

In the theta band, (Figure 2.8), Average coherence between the temporal/occipital regions was found to be significantly different between the two groups. All other differences were not significant. Based on appearance, average coherence was elevated between the frontal/parietal regions, the parietal/occipital regions, and the frontal/occipital regions for both groups. The psychogenic group showed higher average coherence between the frontal/temporal, frontal/central, parietal/temporal, parietal/occipital, parietal/central, and temporal/occipital regions. Average coherence between the occipital/central regions appeared to be similar between the two groups.

For the alpha band, (Figure 2.9), average coherence was elevated between the frontal/parietal regions, the frontal/occipital regions, and the parietal/occipital regions. Average coherence between epileptic and psychogenic groups were similar with no significant differences present. However, average coherence appeared to be slightly larger for the epileptic group between the frontal/parietal, frontal/occipital, parietal/temporal, temporal/occipital, and temporal/central regions.

For the beta band, (Figure 2.10), high average coherence was observed between the frontal/parietal regions, the frontal/occipital regions, and the parietal/occipital regions. Average

coherence between epileptic and psychogenic groups were similar with no significant differences present. However, average coherence appeared to be slightly larger for the epileptic group between the frontal/parietal, frontal/occipital, parietal/temporal, parietal/occipital, temporal/occipital, and temporal/central regions.

For the gamma band, (Figure 2.11), average coherence was largest between the frontal/parietal regions and the parietal/occipital regions. The epileptic group showed higher average coherence in the frontal/parietal, frontal/occipital, and parietal/temporal region pairs. The psychogenic group showed higher average coherence in the parietal/occipital, parietal/central, and temporal/central region pairs. No significant differences in average coherence were found for the gamma band.

In the delta and theta neural frequency bands, 3 of 10 region pairs tested were found to have significant differences between the epileptic and psychogenic groups for average coherence. The alpha, beta, and gamma neural frequency bands were not found to have significant differences between groups for average coherence.

2.3.3 Cross Approximate Entropy

2.3.3.1 C-ApEn: All 18 subjects

Cross approximate entropy between each region pair in both directions were compared between epileptic and psychogenic groups using an independent samples t-test (H_o: $No\ differernce\ in\ C-ApEn\ between\ ES\ and\ PNES$). This is shown in Figure 2.12 and Figure 2.13. See Appendix C for data normality and outlier results.

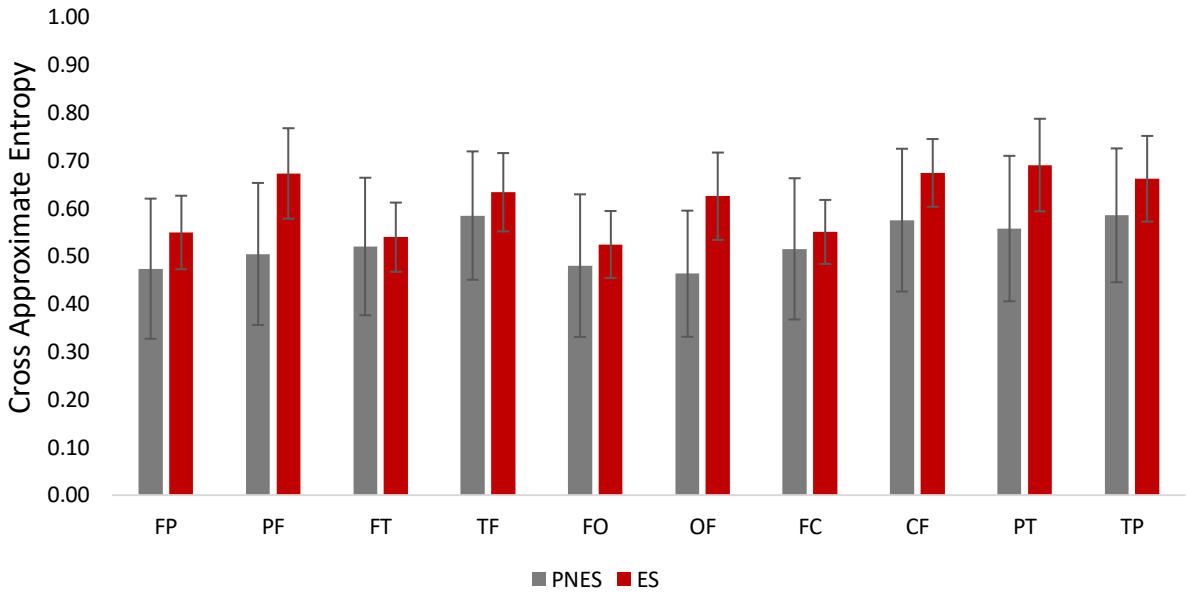

Figure 2.12. Average and standard error of the Cross Approximate Entropy: 1st 10 regions

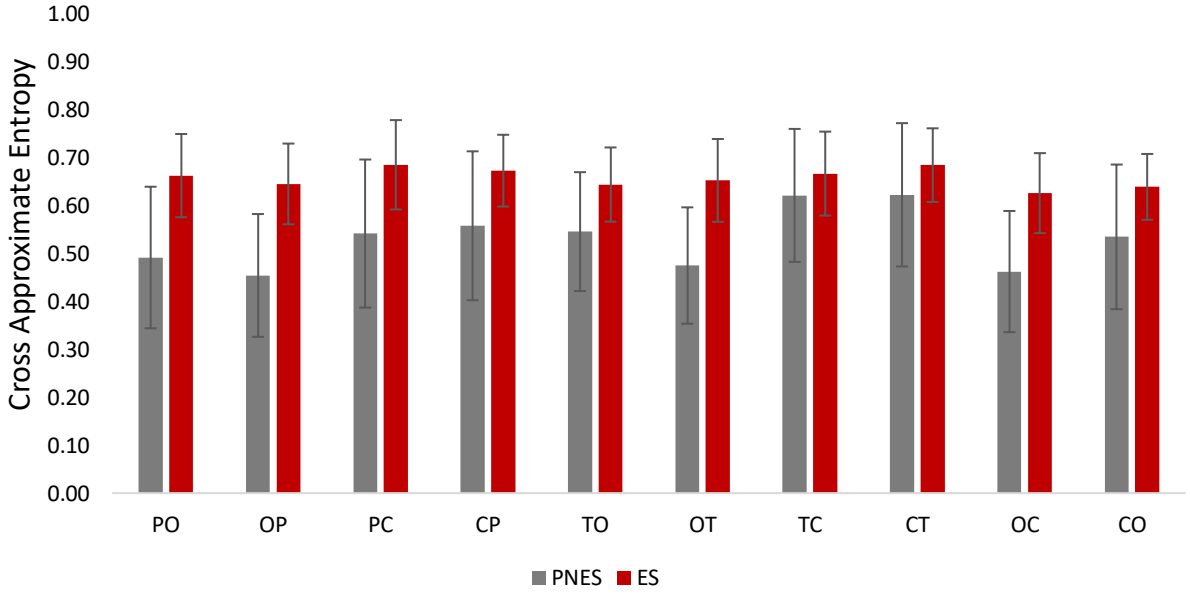

Figure 2.13. Average and standard error of the Cross Approximate Entropy: 2nd 10 regions

From Figures 2.12 and 2.13, average C-ApEn was greater for the epileptic group than the psychogenic group between all region pairs. However, significant differences in C-ApEn were not identified. The lowest average value of C-ApEn for the psychogenic group was between the

occipital/parietal region pair, while the lowest average value of C-ApEn for the epileptic group was between the frontal/occipital region pair. The largest average value of C-ApEn for the psychogenic group was between the central/temporal region pair, while the largest average value of C-ApEn for the epileptic group was between the parietal/temporal region pair. Average C-ApEn did not vary greatly across region pairs.

2.3.3.2 C-ApEn: Subjects 8 and 13 Removed

Subjects 8 and 13 were consistent outliers in C-ApEn between region pairs and were thus removed from the analysis. The independent samples t-test was repeated to compare C-ApEn between epileptic and psychogenic groups (H_o: $No\ differernce\ in\ C-ApEn\ between\ ES\ and\ PNES$). This is shown in Figure 2.14 and Figure 2.15. See Appendix C for data normality and outlier results. A * indicates significance for p<0.10 and ** indicates significance for p<0.05. See Appendix C for data normality and outlier results.

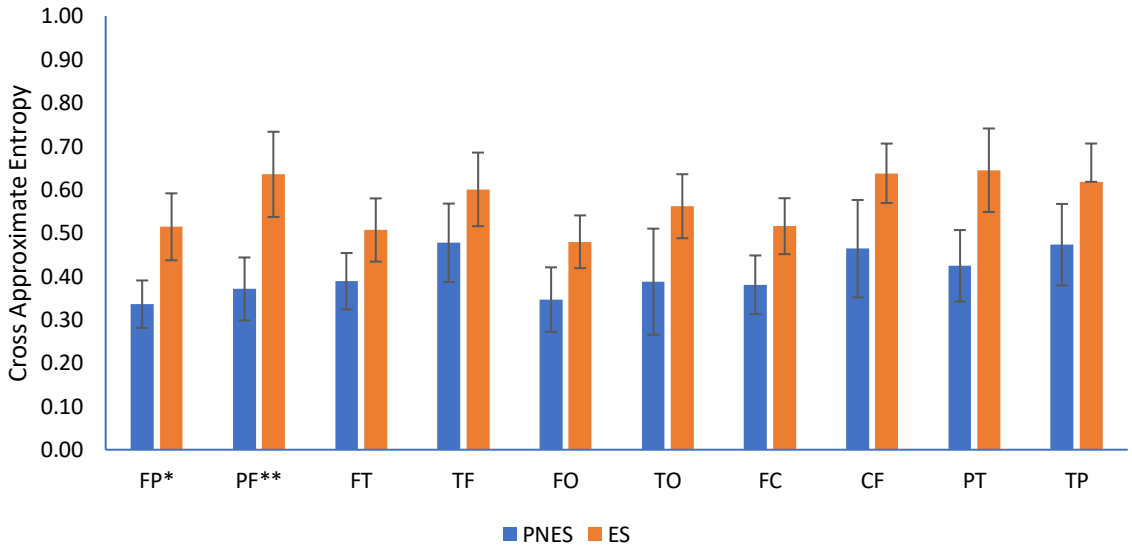

Figure 2.14. Average and standard error of the Cross Approximate Entropy: 1st 10 regions – Subjects 8 and 13 removed

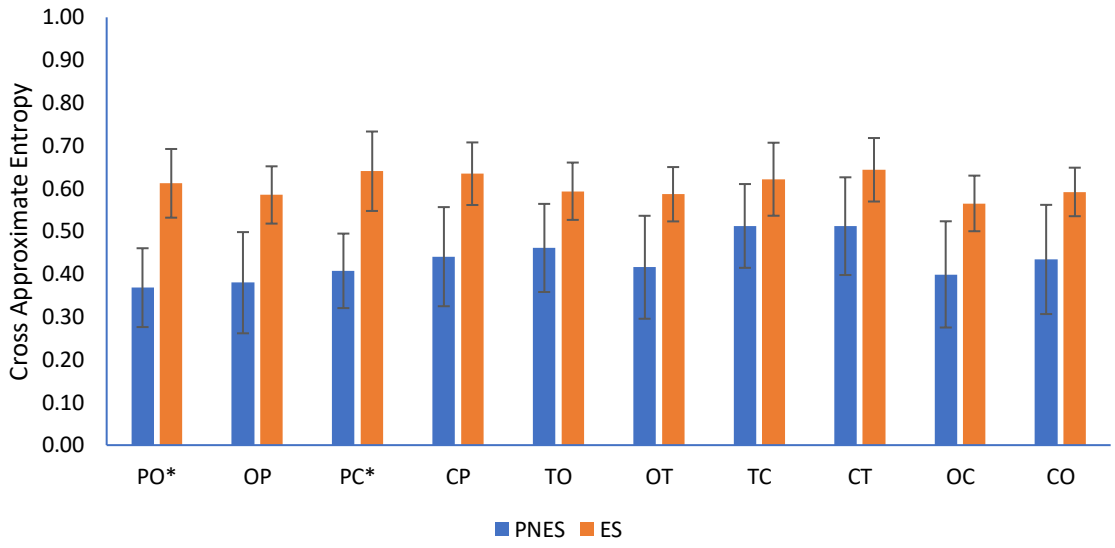

Figure 2.15. Average and standard error of the Cross Approximate Entropy: 2nd 10 regions – Subjects 8 and 13 removed

Removal of subjects 8 and 13 from the analysis improved normality and decreased the presence of outliers in the C-ApEn datasets (Appendix C). From Figure 2.14 and Figure 2.15, the epileptic group continued to show larger C-ApEn between all region pairs. The independent samples t-test results found significant differences between epileptic and psychogenic groups for average C-ApEn between the frontal/parietal, parietal/occipital, and parietal/central region pairs at a significance level of 0.10, and for average C-ApEn between the parietal/frontal region pair at a significance level of 0.05.

2.3.3.3 C-ApEn Time Analysis between Parietal and Central Regions

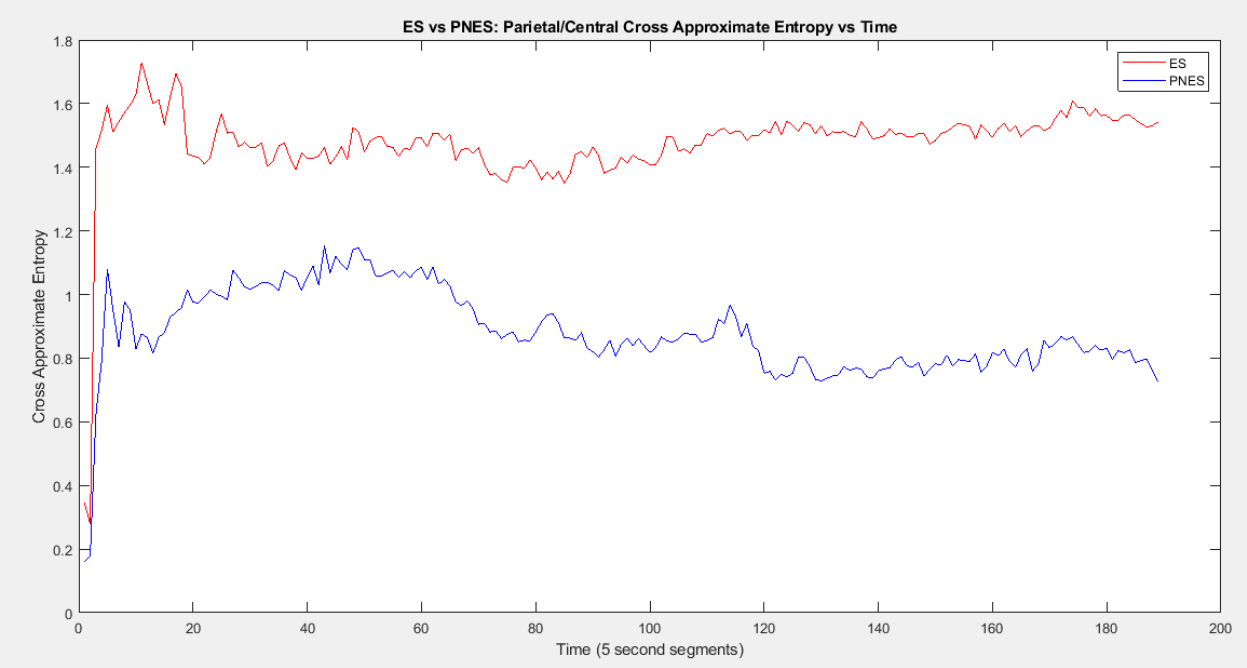

Figure 2.16. Cross Approximate Entropy between parietal and central regions over time using 5 second windows for ES and PNES groups

Figure 2.16 shows C-ApEn values for 5 second intervals over all time for EEG recordings between the parietal and central brain region pair for one subject in the ES group and one subject in the PNES group. A large increase in C-ApEn towards the beginning of the EEG recording can be seen for both ES and PNES groups. C-ApEn remained lower for the PNES group over the full length of time in comparison to the ES group. Visual inspection of C-ApEn over time did not allow for obvious detection of seizure events.

2.4 Discussion

PNES are seizures that appear similar in outward symptoms to epileptic seizures but lack the underlying neurological etiology [2]. Currently, differentiating between PNES and ES is done using video EEG to monitor the patient's brain activity and outward physical behavior during a seizure. This method requires a specialist's interpretation of the EEG signals to identify epileptic activity and relies on their ability to differentiate between non-normal EEG signals and signal artifacts due to external and physiological noise. Though PNES lack the neurological features of ES, visual assessment of EEG signals can often fall short, and patients who experience psychogenic seizure events are frequently misdiagnosed as "epileptic" and are treated ineffectively with AEDs before a proper diagnosis is made [2]-[5]. In fact, accurate diagnosis can take many years, resulting in stress and suffering for patients, caregivers, and physicians [4].

Various signal processing techniques, including time-frequency and information theoretic measures have been applied to EEG signals to detect, classify, and predict epileptic events [6]–[14], [24]. However, few of these techniques have been implemented for the purpose of finding differences between EEG signals recorded from patients who experience PNES from patients who experience ES. Whether or not EEG signals from these two groups of patients can be effectively differentiated using signal processing techniques alone remains unclear. Identification of a biomarker to differentiate between PNES and ES using EEG analysis will facilitate the development of new diagnostic techniques and may improve delays in the diagnostic process for patients suffering from PNES. In this study, surface EEG recordings from 9 patients who experience PNES and 9 patients who experience ES were analyzed using MSC and C-ApEn as measures of neural connectivity between regions of the brain.

For the current study, both MSC and C-ApEn findings suggest differences in brain region connectivity in psychogenic patients versus epileptic patients. Previous studies have indicated that both groups show altered network connectivity among brain areas in comparison to healthy subjects, yet differences in network connectivity between psychogenic and epileptic groups were not as easily identified [4]. Additionally, a few studies have sought to find differences in connectivity within the neural frequency bands and have thus far been unsuccessful in differentiating between the two groups [4], [11].

MSC results were isolated into the neural frequency bands for all region pairs to allow for evaluation of differences between ES and PNES. Average MSC for each region pair within each frequency band were analyzed using an independent samples t-test to compare epileptic and psychogenic groups. Higher frequency band activity has been implicated in epileptic disorders [11], [21]. Additionally, previous studies have sought to find differences in network connectivity within the higher frequency bands between epileptic and psychogenic groups with limited success [11], [21]. The results of this study did not identify differences in average coherence between the two groups for the alpha, beta, and gamma higher neural frequency bands. In contrast, significant differences were identified in the delta (0.5-4Hz) and theta (4-8Hz) lower frequency bands. In the delta band, average coherence between the frontal/central regions, parietal/central regions, and the temporal/occipital regions were found to be significantly different between the epileptic and psychogenic groups, with the epileptic group having lower average coherence than the psychogenic group. In the theta band, average coherence between the temporal/occipital regions was found to be significantly different between the epileptic and psychogenic groups, with the epileptic group having lower average coherence than the psychogenic group.

Directed C-ApEn between all brain regions from epileptic and psychogenic groups were compared using independent samples t-tests. Initial analysis of C-ApEn results revealed no significant differences between the two groups. Two subjects were identified as majority outliers in the C-ApEn datasets. These subjects were removed from the C-ApEn datasets and the analyses were repeated between groups. The results of the independent samples t-test revealed significant differences in average C-ApEn for the frontal/parietal, parietal/frontal, parietal/occipital, and parietal/central region pairs between the two groups with epileptic group having higher average C-ApEn than the psychogenic group.

Studies have indicated that patients who experience PNES show elevated connectivity between areas involved in emotional control and movement [22], [23]. The frontal and temporal lobes of the brain are largely responsible for emotional/voluntary movement and behavior, respectively [24]. In epileptic patients, studies have found that changes in connectivity are most often observed in the temporal and limbic lobes [25]. The present MSC findings indicate stronger connectivity in both the frontal and temporal regions between select region pairs for the PNES group in comparison to the ES group. C-ApEn findings indicate stronger connectivity in the frontal and parietal regions between select regions pairs for the PNES group in comparison to ES group. Furthermore, the most significant difference found for C-ApEn was between the frontal and parietal regions in the direction from parietal to frontal. This suggests that the directionality of information flow may be important in distinguishing the two groups. Limbic lobe connectivity was not evaluated in the present study due to the superficial nature of surface EEG measurements.

Analysis of MSC and C-ApEn revealed differences between epileptic and psychogenic groups. Both measurements found connectivity between the parietal and central regions to be

significantly different between the two groups. Previous research has found that there are changes in connectivity before and after seizure events in epileptic patients [36]. An additional analysis of C-ApEn over time was implemented between the parietal and central regions for one subject from each group. The time analysis revealed C-ApEn between the parietal/central region pair was lower in the PNES group over all time. This result agreed with the single value C-ApEn analysis. Visual inspection of how C-ApEn changed over time did not reveal obvious patterns to indicate when seizure events occurred and therefore, connectivity changes during seizure events were not ascertained. This suggests a more in depth analysis of C-ApEn over time is required to isolate seizure events and evaluate connectivity changes. Interestingly, C-ApEn between the parietal/central region pair showed a large increase following the beginning of the EEG recordings for both PNES and ES subjects. C-ApEn values held more steadily for the remainder of the EEG recording. This finding highlights the importance of the additional time analysis for C-ApEn to observe connectivity changes over time and to prevent loss of relevant information.

MSC and C-ApEn significant findings did not agree for the two measurements for all other region comparisons. This could be explained in that MSC and C-ApEn are inherently different measures. MSC is a time-frequency measure of the linearity of phase relationship between two signals, while C-ApEn is a non-linear time domain measure of signal complexity. The computation time of the C-ApEn algorithm is extremely long for large data sets. C-ApEn provided a much less detailed analysis of neural connectivity in comparison to the additional frequency analysis provided by MSC, which is less computationally heavy. However, C-ApEn does provide the benefit of directionality, which MSC cannot provide.

This study was limited by a small sample size of epileptic and psychogenic patient EEG recordings. A larger sample size would likely improve the normality of the MSC and C-ApEn

results and allow for the ability to validate the present MSC and C-ApEn findings. The EEG data used for this study had limited information concerning when signal events occurred. The analysis would benefit from more a more detailed description of the EEG signals from each patient including time markers for when events occurred (psychogenic, epileptic, signal artifacts, etc.). Additionally, recordings from each patient were highly variable. Some patients were recorded during psychogenic or epileptic events, while some patients were recorded during normal wakefulness or sleep. A more uniform set of data would reduce the presence of outliers in the MSC and C-ApEn results and allow for a more robust comparison between the two groups. Future studies should seek to verify the findings of this study through a more in depth connectivity analysis, particularly in the delta and theta frequency bands and between the region pairs found to be significant for MSC. A C-ApEn analysis should be implemented over time to investigate how connectivity changes between brain regions throughout the EEG recordings. Though MSC and C-ApEn are well established connectivity measures, additional connectivity measures would benefit this study. EEG recording conditions should be more highly controlled and the sample size of the data should be increased. Additionally, a set of normal EEG recordings from healthy subjects implemented as a control would be useful to establish how connectivity in epileptic and psychogenic patients differs from connectivity in normal patients.

2.5 Conclusion

In this study, surface EEG signals from two patient groups, epileptic and psychogenic, were analyzed using C-ApEn to investigate differences in neural connectivity between regions of the brain (frontal, parietal, temporal, occipital, and central), and MSC to investigate differences in neural connectivity between regions of the brain within the neural frequency bands (delta: 0.5-

4Hz, theta: 4-8Hz, alpha: 8-13Hz, beta: 13-30 Hz, and gamma: 30-100Hz). Although previous studies reported inconclusive findings regarding neural connectivity differences between epileptic and psychogenic groups, this study identified significant differences. For both C-ApEn and MSC measures, epileptic and psychogenic patient groups were compared using an independent samples t-test. The statistical analysis concluded that average C-ApEn was greater, indicating lower connectivity, in the epileptic group between the frontal/parietal, parietal/frontal, parietal/occipital, and parietal/central region pairs, and that average MSC was lower, indicating lower connectivity, in the epileptic group in the delta band (frontal/central, parietal/central, and temporal/occipital) and the theta band (temporal/occipital). Both MSC and C-ApEn found connectivity between the parietal/central regions to be significantly lower for the epileptic group.

The current study would benefit from a larger sample size and a more well defined recording protocol to reduce variability within groups. Future research should consider investigating neural connectivity differences between groups using additional analysis techniques with a focus on the significant interactions identified in this study. The results of this study suggest potential areas of brain region interactions that could act as biomarkers for PNES and ES differentiation and may be useful during the diagnostic phase.

Chapter 3. Extended Review of Literature and Extended Methodology

3.1 Extended Review of Literature

3.1.1 Epileptic Seizures

In general, seizures are referred to as paroxysmal events due to their involuntary and abrupt nature. The term epileptic seizure has been defined by the International League Against Epilepsy (ILAE) as "a transient episode of signs/or symptoms due to abnormal or synchronous neuronal activity in the brain" [1], [17]. The signs and symptoms exhibited during an epileptic seizure are highly variable and may include impaired or lost consciousness and abnormal events in some or all the sensory, motor, autonomic, or psychic modalities. These changes can be subtle (e.g. minor sensations) or severe (e.g. large involuntary motor movements) in nature [24]-[28].

Epileptic seizures occur in many patients suffering from a range of disorders associated with seizures. Patients diagnosed with epilepsy constitute the largest subgroup who experience epileptic seizures. A diagnosis of epilepsy requires recurrent and unprovoked epileptic seizure events over a period greater than 24 hours and/or an epilepsy related syndrome [17], [27]. In epilepsy patients, the causes of epileptic seizures have been separated into six distinct categories: (1) structural – an abnormality in the brain anatomy, (2) genetic – family history or genetic variants, (3) infectious – chronic or resolved infection, specific to patients with epilepsy, (4) metabolic – metabolic imbalance, (5) immune – auto-immune disease, and (6) unknown – cause is uncertain [24]. Additional forms of epileptic seizures are defined for patients who do not fit into the epilepsy cohort. These include solitary unprovoked epileptic seizures, febrile seizures, neonatal seizures, and provoked or acute symptomatic seizures [27]. Epileptic seizures that do not originate from epilepsy are summarized in Table 3.1.

Table 3.1. Additional Types of Epileptic Seizure [27]

Seizure Type	Description
Solitary unprovoked epileptic seizures	Seizure/s occurring within a 24 hour period or a single seizure event. Seizure events are isolated; they do not reoccur.
Febrile seizures	Seizures occurring in infants and young children. Rectal temperatures measure at least 101F. There is no history of previous unprovoked seizures and no comorbid central nervous system infection.
Neonatal seizures	Seizures occurring in infants who are less than 28 days of age.
Provoked or acute symptomatic seizures	Seizures associated with an acute, systemic, or toxic factor affecting the central nervous system. This includes "(infection, stroke, cranial trauma, intracerebral hemorrhage, or acute alcohol intoxication or withdrawal". These seizures are not associated with long term abnormalities in the brain.

Basic classification of epileptic seizures is centered on seizure onset which refers to the originating location in the brain. Seizure onsets can be focal, generalized, or unknown. A focal onset refers to a seizure that originated from a localized region in the brain. A generalized onset involves both the right and left hemispheres of the brain. An unknown onset means the region of seizure origination is unknown [17]. Seizures can be further classified according to the expanded classification defined by the ILAE (Figure 3.1).

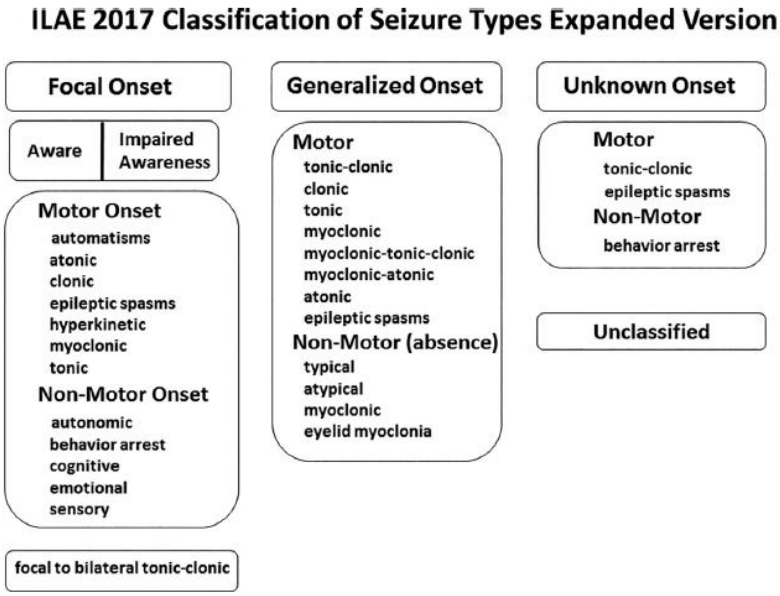

Figure 3.1. ILAE Seizure Classification [17]

The ILAE seizure classification provides detailed seizure categories within the type of seizure onset. Focal onsets are first classified with reference to awareness, followed by motor vs. non-motor presentation. Additionally, a focal onset seizure that shifts to a generalized seizure is labeled as focal to bilateral tonic-clonic. Generalized and unknown onset seizures are evaluated for motor vs. non-motor presentation, with unknown seizures sometimes being categorized as unclassified [17]. The level of detail for seizure classification is determined by the amount of available information pertaining to the seizure event. If a classification level is unknown it is omitted from the seizure type label.

3.1.2 Psychogenic Nonepileptic Seizures

Psychogenic nonepileptic seizures (PNES) are paroxysmal events that resemble epileptic seizures in movements, sensations, and/or experiences but lack clinical evidence for epilepsy [3], [5]. As the term “psychogenic” implies, psychogenic nonepileptic seizures are psychological in

origin and lack the characteristic epileptic discharges that are observed during epileptic seizures. The psychological nature of PNES is the primary difference between PNES, ES, and other nonepileptic events [29]. PNES have been diagnostically classified as dissociative or somatoform disorders and are thought to be a stress response that can be physical, emotional, or social in nature [3], [10]. Brown and Reuber summarized four models to define the origin of psychogenic seizure disorders. The models classify PNES as a psychological response caused by (1) a dissociative event, (2) a hard-wired behavioral tendency or tendencies, (3) a somatoform event, or (4) a learned behavior [30]. The four models are described in Table 3.2.

Table 3.2. The Four Models of PNES Disorders [30]

Model	Description
Dissociative Response	A dissociation or separation of memories and/or mental function. This can be due to previously traumatic events that reoccur for the patient as sensory and motor flashbacks. This suggests a close link to post traumatic stress disorder (PTSD).
Hard-wired Response	An innate behavioral tendency that results as a response to stress or a threat. This is thought to be a protective mechanism and/or serve additional biologic functions. This response is also linked to PTSD. The occurrence of PNES is proposed as an altered state that shares similarities with a panic attack.
Somatoform Response	A physical manifestation of emotional distress without underlying physical or neurological cause. This may be a defensive response to protect the patient from acknowledging emotional causes while allowing for an outlet of emotional energy. The patient may be unable to recognize their emotional state.
Learned Behavioral Response	A result of conditioning through positive and/or negative reinforcement. This has been observed in households with epilepsy sufferers to which other family members may “learn” the seizure behavior.

The four models described in Table 3.2 attempt to describe the triggers behind PNES, but they fail to account for all cases. Brown and Reuber proposed a singular model called the integrated cognitive model (ICM). This model attempts to universally define the mechanisms behind PNES [31]. In the ICM, PNES are described as an involuntary and automatic response to some sort of trigger where the development of the condition is based on the patient's life experiences. The ICM accounts for differences in PNES between individuals and cultures which is expected due to variation in life events and experiences.

Presentation of PNES typically occurs in patients during early adulthood, but it can also occur in much younger and older patients [2]. Patients with PNES show variation in physical and mental health as well as their responsiveness to treatments [30]. Many patients who suffer from PNES are misdiagnosed and treated for epileptic seizures [3], [5]. The treatment for epileptic seizures includes prescription of an antiepileptic drug (AED). AEDs have not been effective in treating PNES and it has been found that they may worsen the symptoms in patients with PNES. It has been suggested that treatment of PNES should include psychiatric/psychological intervention. Studies have shown that many patients who experience PNES also suffer from additional psychiatric conditions such as depression, anxiety, posttraumatic stress, or other somatoform/dissociative disorders [3].

The signs and symptoms of PNES are widely variable from patient to patient. In addition, the symptoms of PNES and ES share many of the same physical characteristics [2]. Nonetheless, these signs and symptoms have been heavily studied to allow for their distinction. The physical differences between the two seizure types are presented in Figure 3.2.

Table. **Differences in Physical Manifestations of Psychogenic Nonepileptic and Epileptic Seizures**

Factor	Psychogenic Nonepileptic Seizures	Epileptic Seizures
Duration	Prolonged	Briefer (usually <5 min)
Clinical features during episode	Fluctuating	Stereotypic
Time of day	Usually during wakefulness in the presence of an audience	May occur in sleep whether or not anyone is present
Consciousness	Preserved even with generalized motor activity	Usually altered (exception is supplementary motor area seizures)
Onset	Gradual, with slow escalation in intensity	Abrupt
Head movements	More frequently side-to-side	Usually unilaterally turned, with staring expression
Extremity	Out-of-phase movements, unusual posturing	In-phase movements, rhythmic muscle contractions
Vocalizations	Emotional (crying) in the middle or end of episode	Cry at the onset of episode
Eyes	Closed during the episode	May be open during the episode
Pelvic thrusting	Forward direction	Retrograde direction
Incontinence	Rare	May be present
Related injury	Inconsistent with fall	Consistent with fall
Tongue bite	Occasional (usually at the tip)	Common (at the side)
Postictal change	None or brief, even after prolonged generalized convulsive event	Prolonged, with confusion and exhaustion (although maybe absent after frontal lobe seizures)

Figure 3.2. Physical Differences between Psychogenic Nonepileptic and Epileptic Seizures [29]

Some of the hallmark features of PNES include “gradual onset or termination of seizure, pseudosleep, discontinuous, irregular, or asynchronous activity (e.g. side-to-side head movement, pelvic thrusting, opisthotonic posturing, stuttering, and weeping), ictal eye closure with extended unresponsiveness, and postictal whispering”[3], [29]. While there are differences in the physical manifestation between the two seizure types, there is a large amount of variation. This variation in PNES symptoms can make diagnosis more challenging for less experienced clinicians. Additionally, it has been noted that symptoms may vary throughout the course of the patient’s lifetime as the underlying mechanism causing PNES changes and that patients who suffer from PNES may also suffer from ES [30], [32].

The ability to effectively diagnose patients with PNES requires an in depth evaluation of the patient’s symptoms, characteristics, and their seizure events. The most success has been

found with using video EEG which allows for monitoring of both the physical and neurological side effects that occur during a seizure. Patients with an increased frequency of seizure episodes can be monitored using video EEG recordings to capture the physical and electrical activities during an event. Close observation of the patient through video EEG enables clinicians to confirm the absence of ictal or post-ictal activity. This means that if the patient presents with the signs and symptoms of a seizure in the absence of epileptic activity and evidence of a psychological trigger, a psychogenic diagnosis will be given.

Aside from patients who experience a high frequency of PNES, other patients may not be as well suited for video EEG monitoring. In this scenario clinicians must rely on patient and/or caregiver accounts of the event, physical symptoms, and surface EEG recordings alone. Current suggestions on increasing the robustness of the diagnostic process include incorporating psychometric testing, automated classifiers, and neuroimaging in addition to video EEG [4], [33], [34]. Combinational approaches for PNES and ES differentiation are helpful but may create additional work for clinicians and further extend the diagnostic process. Automated classification methods could prove to be the most promising due to their potential for decreasing diagnostic delays and error. However automated methods have thus far been lacking in their effectiveness. This suggests a need for more accurate automated method/s to differentiate between PNES and ES.

3.1.3 Electroencephalogram

Electroencephalography (EEG) is a measure of bioelectric potentials that are representative of the electrical activity in the brain [24], [35]. EEG measurements can be taken via the scalp, the cortical surface, or deeper into the neural tissue. These recordings are referred to as surface EEG, electrocorticogram (ECoG), and depth recording, respectively [35]. The surface EEG is the least

invasive method for recording the brain's electrical activity. Signals recorded at the skin's surface propagate from the cerebral cortex to the scalp and are produced by the summation of low frequency inhibitory and excitatory postsynaptic potentials (IPSPs and EPSPs) from many active neurons. The cerebral cortex is made up of neural tissue and exists at the outermost layer of the cerebrum. The cerebrum is responsible for higher order processing of information associated with sensory and motor function, thinking, decision making, and emotion [24]. The cerebrum is divided into two hemispheres, left and right, which are further divided into four lobes: frontal, parietal, temporal, and occipital. Table 3.3 details the processing functions that correspond to each lobe of the brain.

Table 3.3. Functions of the Lobes of the Brain [24]

Lobe	**Function**
Frontal	Personality, emotions, problem solving, motor development, reasoning, planning, parts of speech and movement
Parietal	Sensation, recognition, perception of stimuli, orientation and movement
Temporal	Recognition of auditory stimuli, speech, perception, behavior, and memory
Occipital	Visual processing

The standard 10-20 international system is the typical protocol for electrode placement and makes use of the skulls anatomical features for reference [35]. The primary features used for electrode placement are called the nasion and inion. The nasion is level with the eyes and lies between the nose and forehead and the inion is a bony protuberance at the base of the skull [24]

The ‘10-20’ values have specific meaning which refer to the physical distances between adjacent electrodes. These distances are either 10% or 20% of the length from the front to back or right to left of the skull [24]. Figure 3.3 shows the standard 10-20 electrode placement with the nasion and inion labeled for reference.

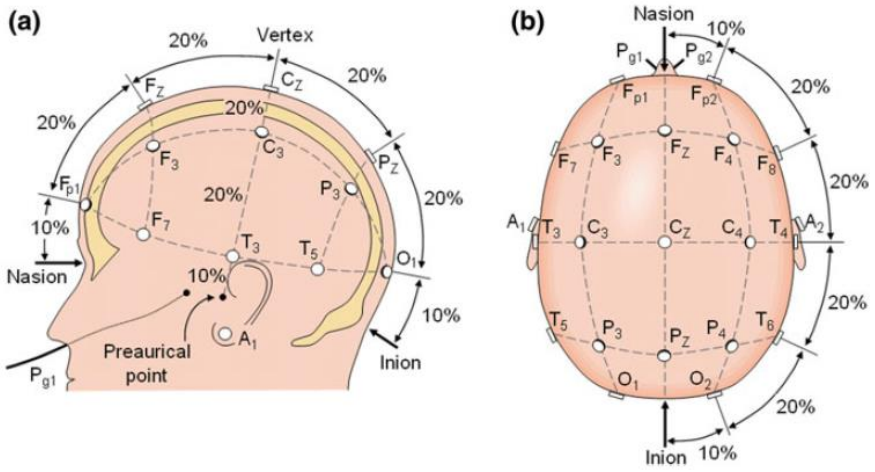

Figure 3.3. Standard 10-20 Electrode Placement [24]

Electrodes are labeled as F (frontal), T (temporal), C (central), P (parietal), and O (occipital). The frontal, temporal, parietal, and occipital labels correspond to the lobes of the brain while the central label corresponds to the coronal plane. A subscript Z (e.g. F_Z) indicates an electrode placed along the midline or sagittal plane. Electrodes with the label A are reference electrodes placed on the mastoid process behind the ears. Numbering of the electrodes is specific to hemisphere with odd numbering on the left hemisphere and even numbering on the right hemisphere [24]. The labeling of the electrodes using the standard 10-20 international system allows for measurement of not only the electrical activity of the brain as a whole, but also of the anatomical regions of the brain as surface EEG signals differ based on their placement and are closely connected to the events within the cerebral cortex [24], [35].

Potentials recorded from surface EEG electrodes result from countless numbers of active neurons and exhibit oscillatory behavior that is often random and aperiodic [24]. The complexity of surface EEG signals like many other bio-signals lends itself to frequency analysis to assess neural function and detect abnormalities in both clinical and research settings. There are five well known frequency bands associated with neural activity in the human brain: delta, theta, alpha, beta, and gamma. Figure 3.4 shows sample EEG waveforms at these frequency bands and the associated cognitive awareness and function.

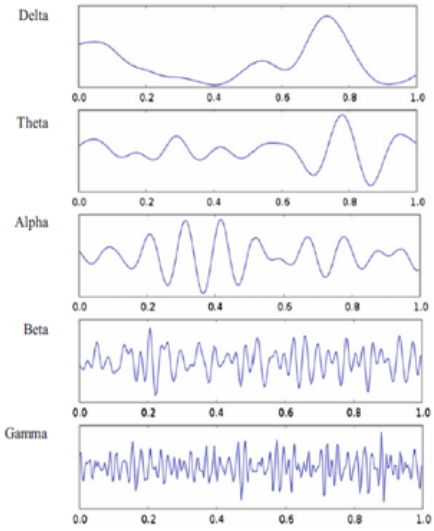

Delta (0.5 – 4 Hz)	Deep sleep, serious brain disorders and the waking state.
Theta (4 – 8 Hz)	Emotional stress (frustration or disappointment and unconscious material), creative inspiration and deep meditation
Alpha (8 – 13 Hz)	Eyes closed or relaxed state, intense mental activity, stress and tension
Beta (13 – 30 Hz)	Strongly engaged, active attention and focus
Gamma (> 30 Hz)	Various cognitive and motor functions

Figure 3.4. EEG Brain Wave Frequency Bands [24]

Normal EEG signals show variation in frequency and amplitude upon changes in cerebral activity [24], [35]. Overall, increases in frequency are associated with increases in brain activity. Similarly, periods of increased mental activity are associated with decreased signal amplitude because activity tends to become less synchronized [35].

Apart from measurement of normal signals, the EEG measurement is one of the main tools used to record abnormal signals and has been central to the detection, monitoring, and

diagnosis of epileptic seizure disorders. Deviations from typical EEG signals indicate abnormal neural activity, such as the uncontrolled hypersynchronous activity that occurs in the epileptic central nervous system [24], [28]. A change from normal brain activity to the onset of a seizure has been frequently characterized by an abrupt change in EEG signal frequency and amplitude, often in the alpha wave frequency band [24]. Activity in the higher frequency bands and rapid spiking sharp waves have also been associated with epileptic EEG recordings [36], [37].

Interpretation of EEG by electroencephalographers can be time consuming and prone to error and has been deemed as an unsatisfactory method due to a lack of standard assessment criteria [24], [37], [38]. It has been suggested that automated systems would be more suitable to the task of EEG evaluation. Many automated algorithms that have been developed in research to analyze EEG data have made us of parametric, nonparametric, time-frequency, and eigenvector techniques to predict, detect, and classify seizure events in epileptic patients [6]–[14], [24], although few of these techniques have been directly applied to the differentiation of neurogenic from psychogenic seizures. Furthermore, many of these techniques have yet to be successfully integrated into the clinical setting [24], [37], suggesting a need for further algorithm development and a well-defined path for clinical implementation.

3.1.4 Time Frequency Analysis and Coherence

Time frequency analysis can provide more information than independent analysis alone because it allows for the simultaneous study of a signals time and frequency content. This type of analysis is especially useful in the investigation of nonstationary processes, such as those of biomedical signals, which are physiological in nature and tend to change with time [38]. Common methods used for time frequency analysis include the periodogram spectrogram, Welch spectrogram, and coherence spectrogram [38]. The spectrogram is a time frequency distribution

which allows for visual interpretation of frequency and time information. Knowledge obtained through time frequency analysis has been used to gain understanding about physiological processes and mechanisms, to detect abnormalities, and to understand relationships between different biomedical signals [19], [39]-[42]. Among the time frequency analysis methods, magnitude squared coherence (MSC) is an especially popular measurement for evaluation of functional neural connectivity. Previous studies have indicated its potential usefulness in the analysis of EEG signals to detect and classify epileptic and non-epileptic seizure events [7], [12], [13], [42].

MSC measures the linear relationship between two time series as a function of frequency. In other words, MSC provides a measure of the similarities in the frequency content of two signals. MSC is effective in the analysis of nonstationary signals because it involves the application of a window to the data. In this way, the window is chosen at a length that allows for the assumption of stationarity of the signal. This also allows for manipulation of time and frequency resolution. Shorter windows improve time resolution, while longer windows improve frequency resolution. Therefore, the window length must also be chosen to create a balance that maintains both the frequency and time information [38].

3.1.5 Approximate Entropy and Cross Approximate Entropy

Approximate entropy (ApEn) provides an information theoretic measure that quantifies the regularity in signals. ApEn was developed by Pincus to evaluate complexity in biosignals arising from both stochastic and deterministic chaotic systems and has proven to be useful in analysis of endocrine, ECG, EEG, and respiration signals [26], [21], [43], [44]. ApEn has four features that make it well suited for biosignal processing: (1) the ability to quantify complexity for short lengths of data, (2) resistance to outliers, (3) resistance to noise, and (4) application to

both chaotic and random signals and to their combination [26]. These features make ApEn especially useful for processing of surface EEG signals that arise from complex neurological processes and are frequently contaminated with noise. It should be noted that ApEn is a biased statistic. This bias is more prominent for shorter lengths of data and therefore care must be taken to ensure that all data being compared is of the same length N [43]. As the length of the data set increases, the bias of the statistic also decreases.

ApEn is a measure of complexity within a particular signal. Cross approximate entropy (C-ApEn) was developed from ApEn as a measure of complexity between two signals. This allows for assessment of independence between signals and more importantly allows for comparison of signals that could arise from processes similar yet distinct in nature or different processes altogether [26]. In this way, C-ApEn provides insight into the relationship between signals from which inter-signal connectivity can be inferred.

The features of ApEn that make it useful for biosignal processing also apply to C-ApEn. Even more, application of C-ApEn has the potential to provide more information that ApEn alone, however its high computational cost has made its implementation less popular in the research community [45]. In any case, previous studies have implemented C-ApEn as a measure of neural connectivity to identify biomarkers in patients with Alzheimer's disease, and to evaluate female hormone levels [15]-[16].

3.2 Extended Methodology

3.2.1 Subject Data

Surface EEG recordings from 18 subjects were provided to Grand Valley State University by the Spectrum Health Office of Clinical Research in conjunction with the Epilepsy Monitoring Unit. Subjects were categorized into two groups based on the incidence of psychogenic or epileptic seizures: 0 (control or psychogenic) or 1 (epileptic). The surface EEG recordings for all patients had a sampling rate of 200 Hz. Length of recording varied from 8.7 minutes to 10.5 minutes. Subject numbers, grouping, and EEG interpretations were provided along with the EEG data . EEG interpretation notes gave limited information about the subject's state during recording (sleep or wakefulness), the presence of seizure activity (psychogenic or epileptic) and artifacts, as well as the suspected type of epilepsy for subjects in the epileptic group. The timing of events was not specified in the patient notes. The EEG interpretations indicate that the surface EEG data from all subjects are representative of a combination of both normal EEG signals and non-normal (psychogenic or epileptiform) EEG signals. Table 3.4 shows the notes provided for each subject.

Table 3.4. Subject Classification and EEG Interpretations

Subject ID	Epileptic or Control Group 0 =Control 1 = Epileptic	EEG Interpretation
1	0	normal wakefulness, muscle artifact, eye movement artifact, photic stimulation with normal posterior driving response
2	0	normal stage II sleep with a single, brief arousal (arousal-associated muscle artifact during the arousal); at other times in the record, the patient has temporal lobe slowing, but this slowing was not evident in this sleep sample.
3	0	normal stage II sleep with minimal muscle artifact
4	0	normal wakefulness with one brief psychogenic nonepileptic convulsive event with muscle and movement artifact
5	0	normal stage II sleep with brief arousal (arousal-associated muscle artifact during the arousal). Has left temporoparietal slowing in wakefulness
6	0	normal wakefulness with muscle artifact, photic stimulation, and hyperventilation
7	0	wakefulness with left temporal slow waves, also muscle artifact
8	0	normal wakefulness with psychogenic event and copious muscle artifact
9	0	normal wakefulness, photic stimulation, hyperventilation with prominent normal hyperventilation response
10	1	left temporal spike-wave and sharp and slow wave discharges; otherwise unremarkable wakefulness; [suspected left temporal lobe epilepsy]
11	1	normal wakefulness except for a brief burst of nonspecific, sharply-contoured frontal theta; eyes open throughout; [poorly lateralized, poorly, poorly localized focal epilepsy]

12	1	stage II sleep, REM sleep, no epileptiform activity or other abnormality; [patient does have focal, extratemporal epilepsy]
13	1	wakefulness and light drowsiness, largely unremarkable except for frequent left temporal slow waves and occasional left temporal sharp waves; [focal epilepsy of left hemispheric origin]
14	1	stage II sleep with right frontotemporal spikes and sharp waves as well as right anterior temporal slow waves; [right temporal lobe epilepsy]
15	1	stage II sleep with frequent interictal discharges (left centroparietal spikes and sharp waves > left anterior temporal sharp waves > left occipital spikes) and left > right hemispheric slow waves; [left temporoparietal epilepsy]
16	1	wakefulness with right greater than left temporal lobe slow waves, no epileptiform activity; [prior left temporal lobe epilepsy, rare seizures following left temporal lobe surgery]
17	1	stage II sleep, midline central spike-wave discharge; [focal epilepsy or right posterior quadrant origin]
18	1	stage II sleep, right hemispheric slowing; [independent right and left hemispheric focal seizures]

3.2.2 Data Analysis

All surface EEG signals were analyzed using non-parametric information theoretic and time-frequency measures to assess network connectivity between regions of the brain using MATLAB 2019a. Five brain regions were selected for analysis: (1) Frontal, (2) Parietal, (3) Temporal, and (4) Occipital corresponding to the lobes of the brain, as well as a (5) Central region that corresponds to the positional placement of recording electrodes along the coronal plane. A total of 10 pairs of regions were evaluated. The region pairs are shown in Table 3.5.

Table 3.5. Region Pairs of Interest

Region Number	Region Pair
1	Frontal / Parietal
2	Frontal / Temporal
3	Frontal / Occipital
4	Frontal / Central
5	Parietal / Temporal
6	Parietal / Occipital
7	Parietal / Central
8	Temporal / Occipital
9	Temporal / Central
10	Occipital / Central

Frequency analysis further allowed for evaluation of connectivity between brain regions in the neural frequency bands: Delta (0.5 – 4 Hz), Theta (4-8 Hz), Alpha (8-13 Hz), Beta(13-30 Hz), and Gamma (30-100 Hz).

3.2.2.1 Preprocessing

EEG signals often contain artifacts from many sources including powerline interference, blinking, muscle contraction, and relative displacement between electrodes and patients. One must be careful in the steps taken to remove this noise as to not compromise the integrity of the EEG signal because the energy of such noise often spans the full range of the neural frequency bands (0.5-100Hz) [6]. Powerline interference occurs around 60 Hz and can be easily identified in the signal and removed via filtering. A 2nd order Butterworth notch filter at 60 Hz was applied to the raw surface EEG signals to remove powerline interference. Referring to Table 3.4, the

EEG interpretation notes indicated the presence of muscle artifact noise for many of the subjects. One way to mediate the effect of muscle artifact is through reference averaging to reduce the impact of any channel electrodes carrying excess noise. In this way reference averaging also helps to minimize artifacts from relative displacement between electrodes and patients. A reference average was applied by subtracting the average of all the EEG electrodes from the EEG signal for all subject data.

3.2.2.2 Brain Regions of Interest

The surface EEG data consisted of 23 recording channels based on the international standard 10-20 protocol for EEG electrode placement. EEG signal channels were extracted and grouped according to Table 3.6. The EEG signals were averaged within each group to obtain a single representative time series for each brain region.

Table 3.6. EEG Signal Channels Grouping for each Brain Region

Brain Region	**EEG Signal Channels**					
Frontal	'Fp1'	'Fp2'	'F3'	'F4'	'F7'	'F8'
Parietal		'P3'	'P4'	'P7'	'P8'	
Temporal		'T7'	'T8'	'T1'	'T2'	
Occipital			'O1'	'O2'		
Central			'C3'	'C4'		

3.2.2.3 Magnitude Squared Coherence

Magnitude squared coherence (MSC) is a technique that measures the linear relationship between two time series as a function of frequency. MSC is often calculated as a function of frequency alone, $MSC(f)$, but can also be calculated more robustly as a function of both time and frequency, $MSC(n,k)$. The process for calculating $MSC(n,k)$ begins with computing the short term minimum bias eigentransform (STET) defined by

$$X_l[n,k] = \sum_{m=0}^{M-1} x\left[n+m-\frac{M}{2}\right] V_l[m] e^{-j2\pi mk/M} \qquad (3.1)$$

where $x[n+m-M/2]$ is a the input signal to be evaluated at n time points with percent overlap of $M/2$, $V_l[m]$ is spheroidal sequence of l mutli-taper windows of length M, and k is the frequency index. The STET is computed for both input time series signals to obtain $X_l[n,k]$and $Y_l[n,k]$. The auto power spectra and the cross power spectrum are then computed using the results of the STET:

$$S_{xx} = |\sum_{l=0}^{L-1} X_l[n,k]|^2 \qquad (3.2)$$

$$S_{yy} = |\sum_{l=0}^{L-1} Y_l[n,k]|^2 \qquad (3.3)$$

$$S_{xy} = \sum_{l=0}^{L-1} X_l[n,k] Y_l^*[n,k] \qquad (3.4)$$

$MSC(n,k)$ can then be computed as

$$MSC(n,k) = \frac{|S_{xy}(n,k)|^2}{S_{xx}(n,k) S_{yy}(n,k)} \qquad (3.5)$$

MSC provides frequency correlation results between 0 and 1, revealing the similarity between the frequency content in two signals over time [38]. An MSC value of 0 indicates a non-linear relationship while an MSC value of 1 indicates an ideal linear relationship. The MSC results can be assessed visually using a coherence spectrogram.

An algorithm to compute $MSC(n,k)$ was developed in MATLAB 2019a to evaluate neural connectivity between brain regions in the neural frequency bands. A spheroidal sequence of L = 7 mutli-taper windows with M = 1200 was generated using MATLAB's discrete prolate spheroidal (Slepian) sequences (DPSS) function. Since fs = 200 Hz, the window length, M, was chosen to achieve a time resolution of 6 seconds and a frequency resolution of 0.167 Hz. The number of FFT points was chosen as 1200 to match the window length. The time increment was set to 600 for 50% overlap.

For all subjects, coherence spectrograms were obtained for each region pair spanning the neural frequency bands for the full length of recording. The region pair MSC values were further manipulated to obtain average MSC time series for each of the neural frequency bands. Finally, the time series data was averaged once more to obtain a single coherence value for each region in each neural frequency band. Figure 3.5 illustrates the process that was taken to obtain the final MSC averages.

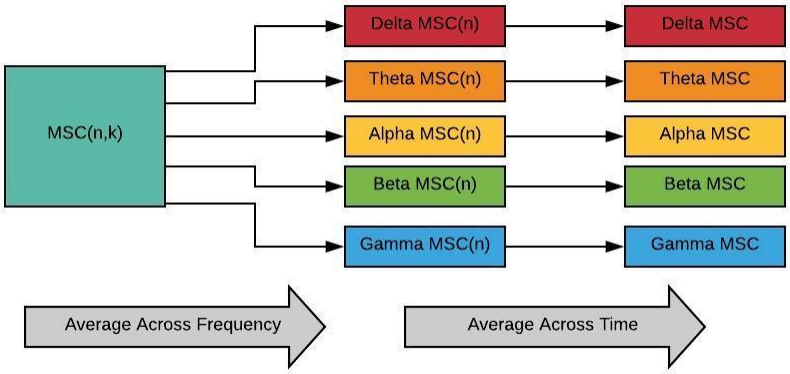

Figure 3.5. Flow Diagram of MSC Average Calculations

3.2.2.4 Cross Approximate Entropy

Cross approximate entropy ($C - ApEn$) is a non-linear directed measure that describes the pattern complexity or similarity between two times series [26]. To understand $C - ApEn$ it is helpful to first understand the approximate entropy ($ApEn$) algorithm, which is used to quantify the complexity of a single time series. $ApEn$ was first proposed by Pincus [20] as a time analysis technique for bio-signal processing. Fusheng et al. provide a detailed definition and interpretation of $ApEn$ and $C - ApEn$ [26] that is summarized below.

As previously stated, $ApEn$ is a statistic that measures the complexity of a single time series $x(n)$ defined by

$$ApEn(m, r, N) = \Phi^m(r) - \Phi^{m+1}(r) \qquad (3.6)$$

where m is the dimension that describes the length of each data block to be compared, r is a threshold that acts as a noise filter, and N is the total length of the data. The computation of $ApEn(m, r, N)$ begins with the definition of the values m and r. As suggested by the literature [20], the value of m is usually chosen as 2 and the value of r is taken as $0.2SDx$ where SDx is the standard deviation of the data $x(n)$. Following, a series of computations are performed at dimension m and then repeated for $m + 1$. The steps of computation and their meaning are described below.

Step 1. Create vectors of length m:

$$X(i) = [x(i), x(i+1), \dots, x(i+m-1), \quad i = 1, N-m+1 \qquad (3.7)$$

For $m = 2,\ X(i)$ is a line segment or two-point pattern, $[x(i)\ \ x(i+1)]$, that joins every two consecutive data points, and for $m = 3,\ X(i)$ is a line segment or three-point pattern, $[x(i)\ x(i+1)\ x(i+2]$, that joins every three consecutive data points.

Step 2. Define the distance as the absolute maximum difference between $X(i)$ and $X(j)$:

$$d[X(i)\ \ X(j)] = \ max_{k=0,m-1}[|x(i+k) - x(j+k)|] \qquad (3.8)$$

Step 3. For a given $X(i)$, find the number of distances, $d[X(i)\ \ X(j)], (j = 1, N-m+1)$ that are $\leq r$:

$$N^m(i) = \#\ of\ d[X(i)\ \ X(j)]\ \leq r \qquad (3.9)$$

The meaning of $N^m(i)$ is then the total number of m-point patterns formed by all consecutive data points in the time series that are close to $X(i)$ within the threshold tolerance of $\pm r$.

Step 4. Compute the ratio of $N^m(i)$ to the total number of all m-point patterns, $(N-m+1)$:

$$C_r^m(i) = \frac{N^m(i)}{N-m+1} \qquad (3.10)$$

The ratio, $C_r^m(i)$, defines the frequency of occurrence of m-point patterns that are close to $X(i)$ within the threshold tolerance of $\pm r$.

***** Steps 3 and 4 are computed for all $i, (i = 1, N-m+1)$.

Step 5. Take the natural logarithm of the ratio, $C_r^m(i)$, and average it over i:

$$\Phi^m(r) = \frac{1}{N-m+1}\sum_{i=1}^{N-m+1} \ln C_r^m(i) \qquad (3.11)$$

$\Phi^m(r)$ represents the average frequency that all m-point patterns in the time series remain close to one another.

Step 6. Repeat steps 1-5 for m+1

Step 7. Compute $ApEn(m, r, N)$ using equation 3.6: $ApEn(m, r, N) = \Phi^m(r) - \Phi^{m+1}(r)$

The meaning of $ApEn(m, r, N)$ for $m = 2$ can be interpreted as the difference between the average frequency that all 2-point patterns in the time series remain close to one another and the average frequency that all 3-point patterns in the time series remain close to one another. This reveals the incidence of new pattern generation when the dimension m decreases from $m = 3$ to $m = 2$ [26]. A larger value of $ApEn(m, r, N)$ indicates a higher degree of new pattern generation and thus higher signal complexity.

The maximum possible value of $ApEn$ is defined by $ln\ k$, where k is the number base of the data sequence [20]. For example, in base 10, the maximum value of $ApEn$ would be $ln\ 10$ or ~ 2.30. In theory, $ApEn = 0$ would indicate a perfectly predictable signal, while $ApEn = \sim 2.30$ would indicate a completely random signal.

Now that $ApEn$ is well understood, a description of the $C - ApEn$ algorithm can be given. $ApEn$ is an auto-comparison that reveals information about one signal's complexity while

$C - ApEn$ is a cross comparison that measures the complexity between two signals. Computation of $C - ApEn$ is easily derived from the steps used to calculate $ApEn$.

For two times series, $x(n)$ and $y(n)$, the length dimension m and the threshold r are kept the same, $(m = 2)$ and $(r = 0.2SD)$. However, in order for the threshold r to be valid for both $x(n)$ and $y(n)$, the two time series must have the same standard deviation. This is achieved by normalizing $x(n)$ and $y(n)$:

$$x'(n) = \frac{x(n) - \overline{x(n)}}{SDx} \qquad (3.12)$$

$$y'(n) = \frac{y(n) - \overline{y(n)}}{SDy} \qquad (3.13)$$

The remaining steps for computation of $C - ApEn$ are described below.

Step 1. Create two sets of vectors of length m:

$$X(i) = [x(i), x(i+1), \dots, x(i+m-1), \quad i = 1, N-m+1 \qquad (3.14)$$

$$Y(j) = [y(j), y(j+1), \dots, y(j+m-1), \quad j = 1, N-m+1 \qquad (3.15)$$

Step 2. Define the distance between vectors as the absolute maximum difference between $X(i)$ and $Y(j)$:

$$d[X(i)\ Y(j)] = max_{k=0,m-1}[|x(i+k) - y(j+k)|] \qquad (3.16)$$

Step 3. For a given $X(i)$, find the number of distances, $d[X(i)\ Y(j)], (j = 1, N - m + 1)$ that are $\leq r$:

$$N_{xy}^{m}(i) = \#\ of\ d[X(i)\ Y(j)]\ \leq r \qquad (3.17)$$

The meaning of $N_{xy}^{m}(i)$ is then the total number of $Y(j), (j = 1, N - m + 1)$ that are close to the m-point pattern formed by $X(i)$ within the threshold tolerance of $\pm r$.

Step 4. Compute the ratio of $N_{xy}^{m}(i)$ to the total number of all m-point patterns, $(N - m + 1)$:

$$C_{xy}^{m}(i) = \frac{N_{xy}^{m}(i)}{N-m+1} \qquad (3.18)$$

The ratio, $C_{xy}^{m}(i)$, defines the frequency of occurrence of the m-point y patterns formed by $Y(j), (j = 1, N - m + 1)$ being within the threshold tolerance of $\pm r$ to the m-point x pattern of a given $X(i)$.

***** Steps 3 and 4 are repeated for all $X(i), (i = 1, N - m + 1)$.

Step 5. Take the natural logarithm of the ratio, $C_{xy}^{m}(i)$, and average it over i:

$$\Phi_{xy}^{m}(r) = \frac{1}{N-m+1}\sum_{i=1}^{N-m+1} \ln C_{xy}^{m}(i) \qquad (3.19)$$

$\Phi_{xy}^{m}(r)$ represents the average frequency that all m-point patterns in $Y(j)$ remain close for all m-point patterns in $X(i)$.

Step 6. Repeat steps 1-5 for m+1

Step 7. Compute $C - ApEn(m, r, N)$*:*

$$C - ApEn(m, r, N) = \Phi_{xy}^{m}(r) - \Phi_{xy}^{m+1}(r) \qquad (3.20)$$

For $m = 2$, the meaning of $C - ApEn(m, r, N)$ can be interpreted as the difference between the average frequency that all 2-point patterns in $Y(j)$ remain close for all 2-point patterns in $X(i)$ and the average frequency that all 3-point patterns in $Y(j)$ remain close for all 3-point patterns in $X(i)$ [26]. Intuitively, this provides the rate of new pattern generation from dimension $m = 3$ to $m = 2$ and thus the cross complexity of the two time series signals $x(n)$ and $y(n)$. A larger value of $C - ApEn$ would indicate higher complexity between the two signals and thus lower connectivity. Because $C - ApEn$ is a directed measure, it also provides a way to assess how connectivity varies based on directionality.

A $C - ApEn$ algorithm was developed in MATLAB 2019a to evaluate neural connectivity between brain regions. The dimension m was chosen as 2 and the threshold r was chosen as $0.2SD$. Each time series was normalized before computing $C - ApEn$. Region pairs were evaluated in both directions, i.e. $C - ApEn$ was computed for 20 cases per subject.

Appendix A. Subject Notes – EEG Interpretations

Table A1. Subject Classification and EEG Interpretations

Subject ID	Epileptic or Control Group 0 =Control 1 = Epileptic	EEG Interpretation
1	0	normal wakefulness, muscle artifact, eye movement artifact, photic stimulation with normal posterior driving response
2	0	normal stage II sleep with a single, brief arousal (arousal-associated muscle artifact during the arousal); at other times in the record, the patient has temporal lobe slowing, but this slowing was not evident in this sleep sample.
3	0	normal stage II sleep with minimal muscle artifact
4	0	normal wakefulness with one brief psychogenic nonepileptic convulsive event with muscle and movement artifact
5	0	normal stage II sleep with brief arousal (arousal-associated muscle artifact during the arousal). Has left temporoparietal slowing in wakefulness
6	0	normal wakefulness with muscle artifact, photic stimulation, and hyperventilation
7	0	wakefulness with left temporal slow waves, also muscle artifact
8	0	normal wakefulness with psychogenic event and copious muscle artifact
9	0	normal wakefulness, photic stimulation, hyperventilation with prominent normal hyperventilation response
10	1	left temporal spike-wave and sharp and slow wave discharges; otherwise unremarkable wakefulness; [suspected left temporal lobe epilepsy]

11	1	normal wakefulness except for a brief burst of nonspecific, sharply-contoured frontal theta; eyes open throughout; [poorly lateralized, poorly, poorly localized focal epilepsy]
12	1	stage II sleep, REM sleep, no epileptiform activity or other abnormality; [patient does have focal, extratemporal epilepsy]
13	1	wakefulness and light drowsiness, largely unremarkable except for frequent left temporal slow waves and occasional left temporal sharp waves; [focal epilepsy of left hemispheric origin]
14	1	stage II sleep with right frontotemporal spikes and sharp waves as well as right anterior temporal slow waves; [right temporal lobe epilepsy]
15	1	stage II sleep with frequent interictal discharges (left centroparietal spikes and sharp waves > left anterior temporal sharp waves > left occipital spikes) and left > right hemispheric slow waves; [left temporoparietal epilepsy]
16	1	wakefulness with right greater than left temporal lobe slow waves, no epileptiform activity; [prior left temporal lobe epilepsy, rare seizures following left temporal lobe surgery]
17	1	stage II sleep, midline central spike-wave discharge; [focal epilepsy or right posterior quadrant origin]
18	1	stage II sleep, right hemispheric slowing; [independent right and left hemispheric focal seizures]

Appendix B. MSC Figures

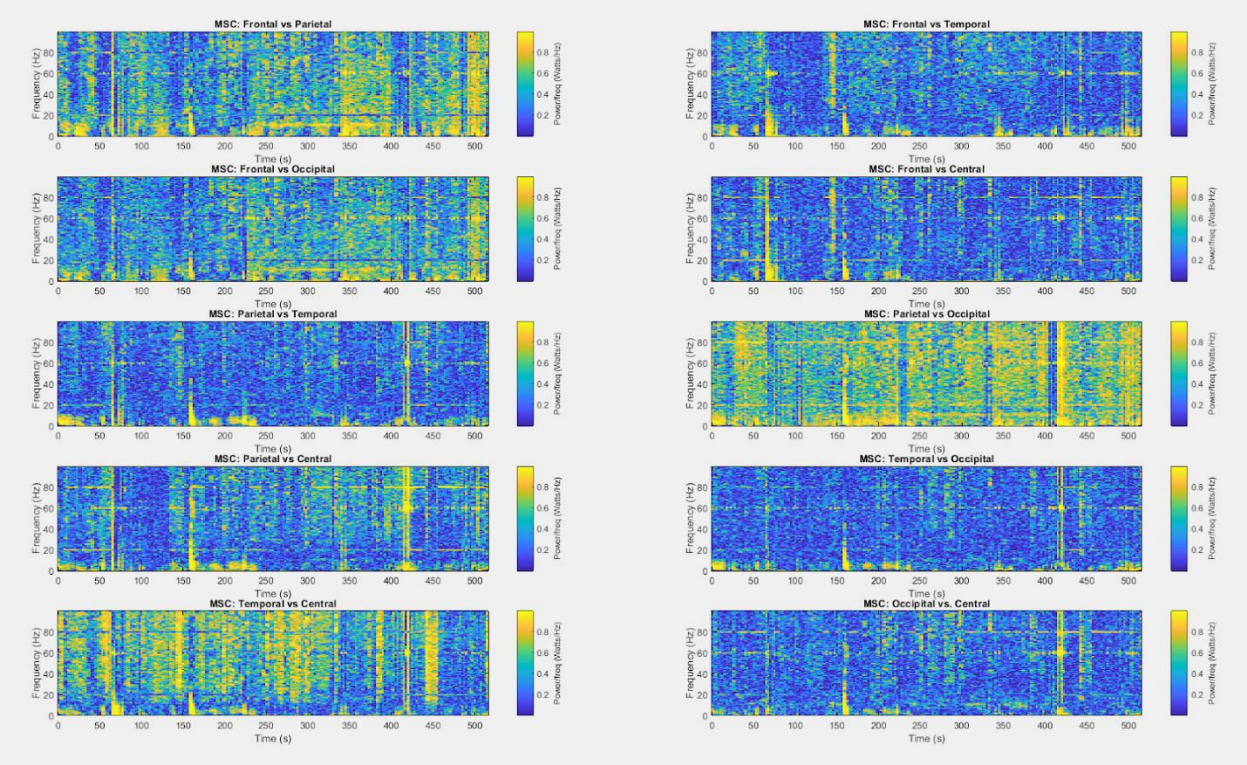

Figure B1. MSC Spectrograms between all region pairs: Subject 1 PNES

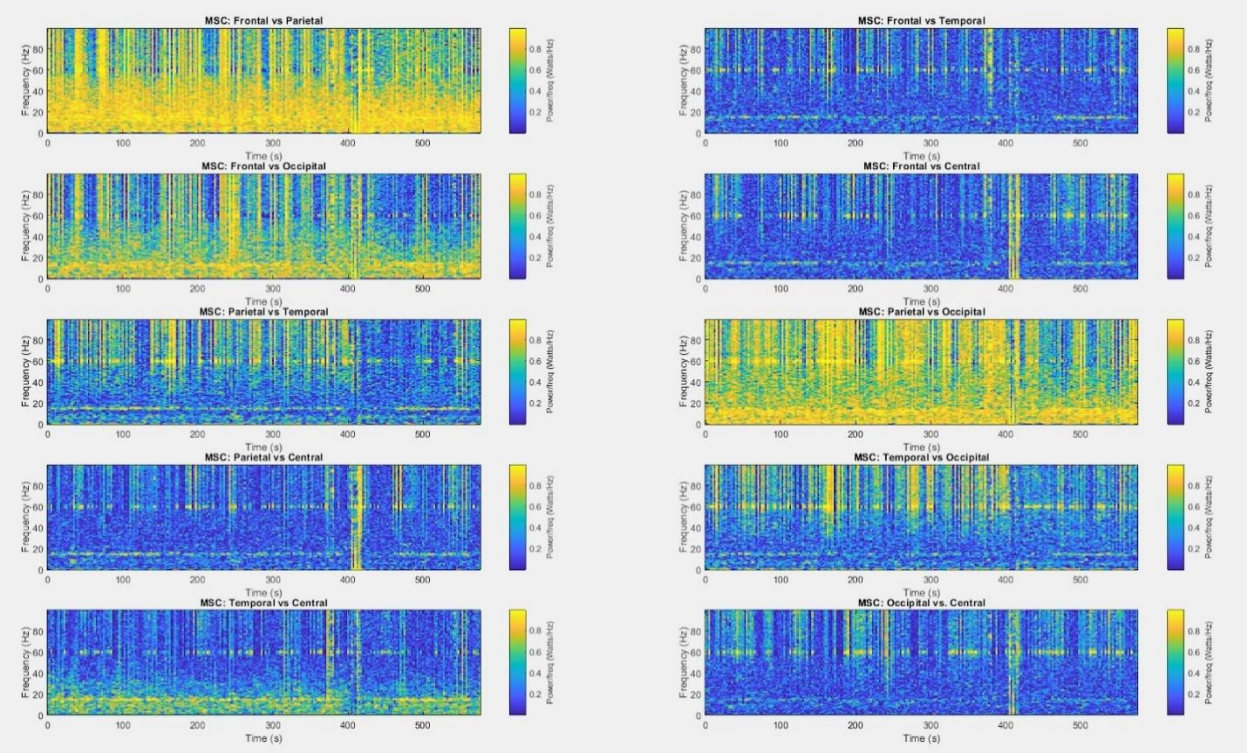

Figure B2. MSC Spectrograms between all region pairs: Subject 2 PNES

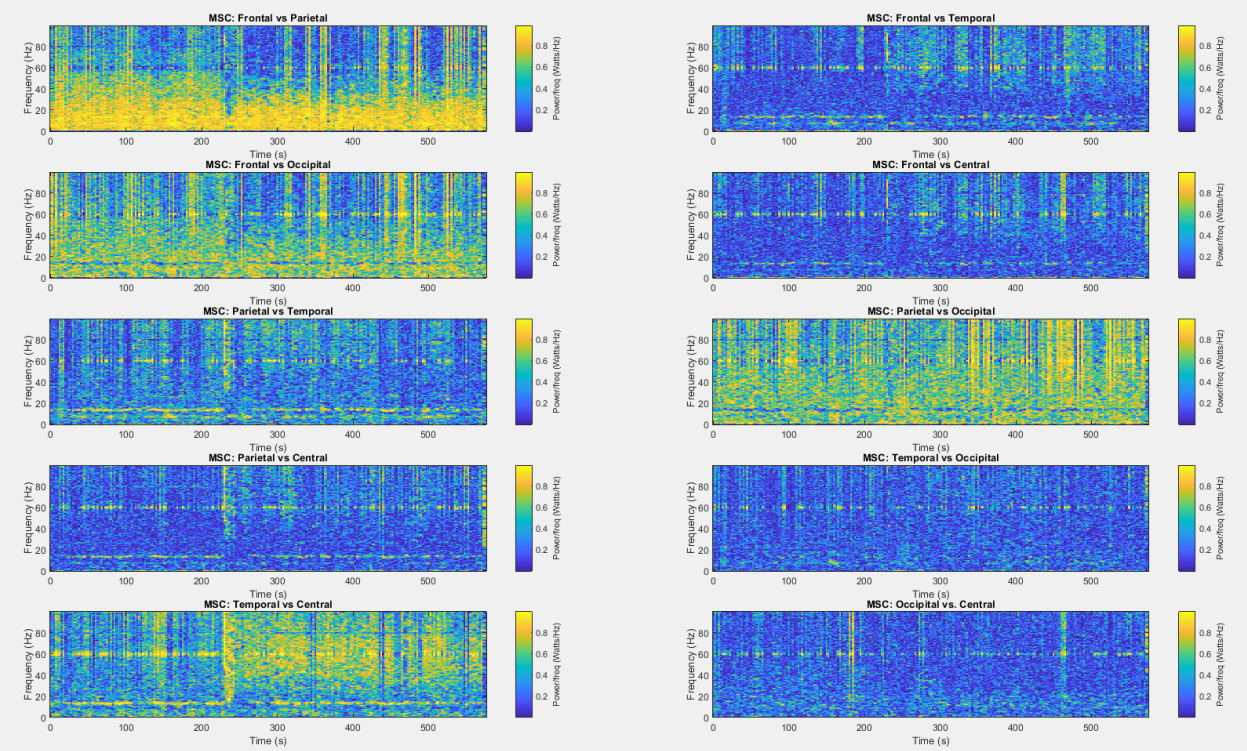

Figure B3. MSC Spectrograms between all region pairs: Subject 3 PNES

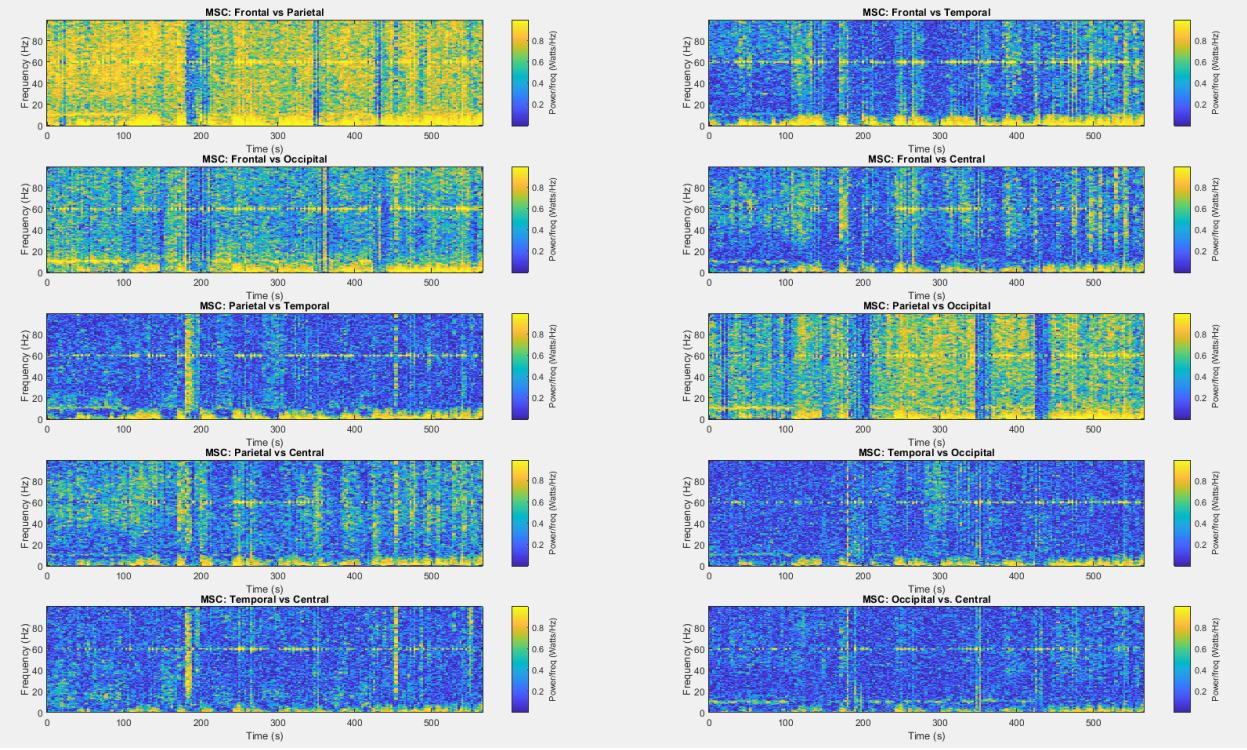

Figure B4. MSC Spectrograms between all region pairs: Subject 4 PNES

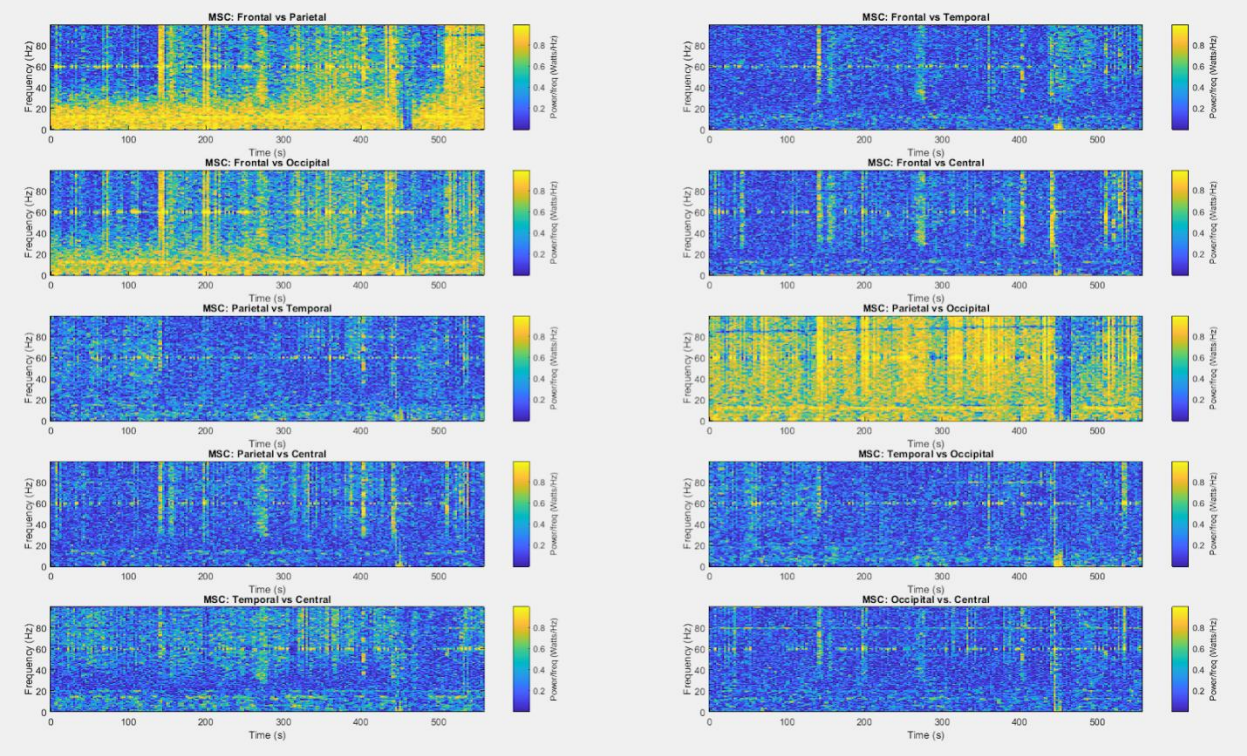

Figure B5. MSC Spectrograms between all region pairs: Subject 5 PNES

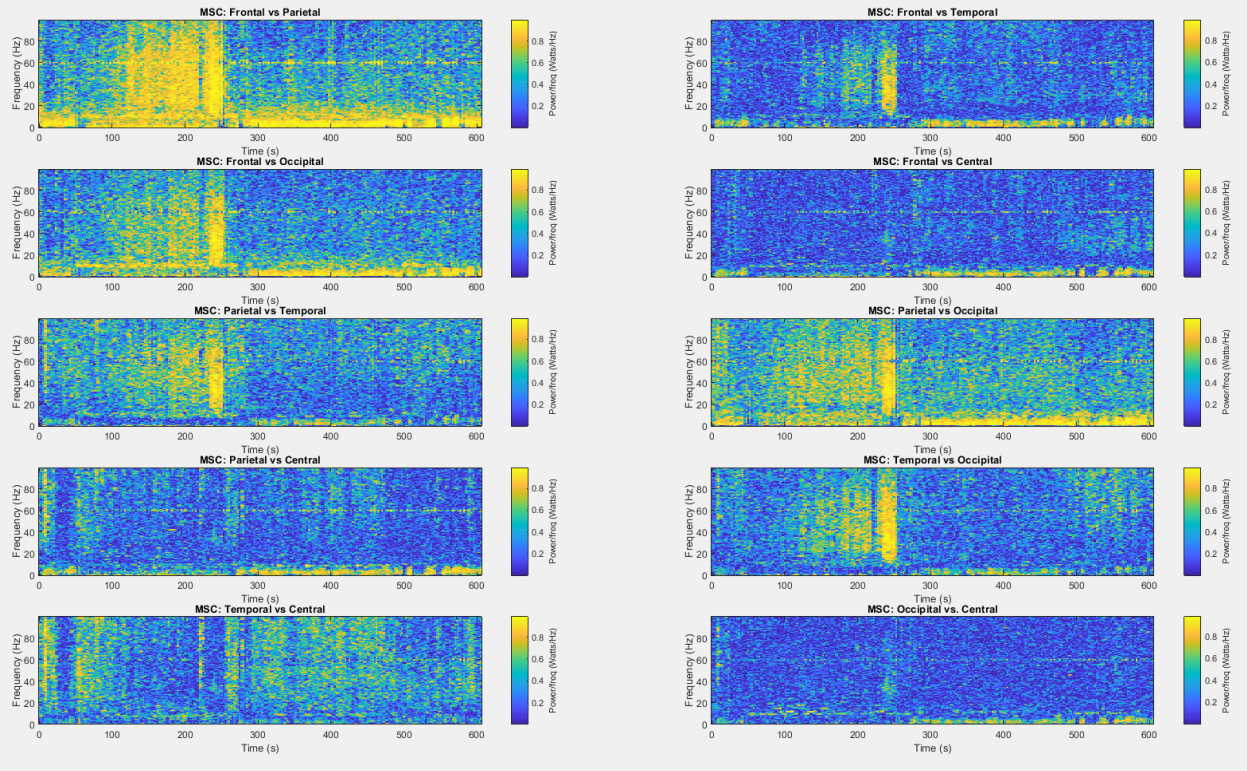

Figure B6. MSC Spectrograms between all region pairs: Subject 6 PNES

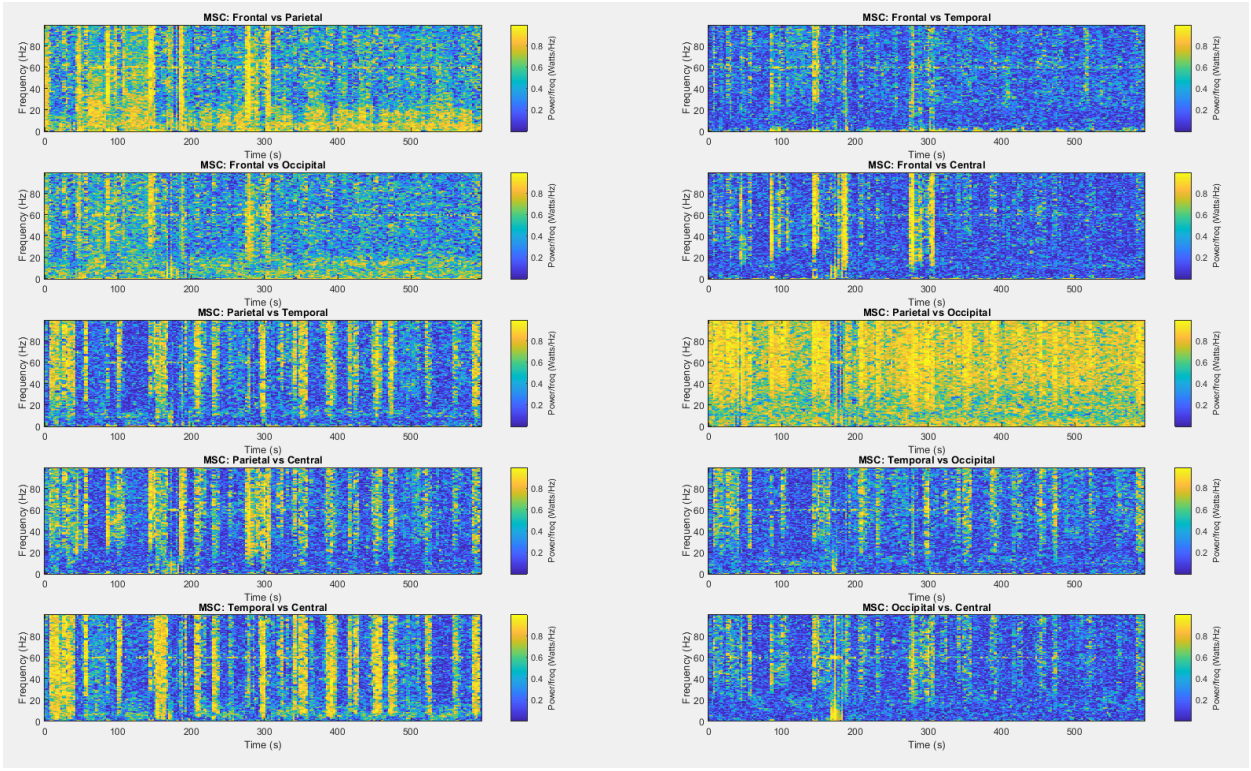

Figure B7. MSC Spectrograms between all region pairs: Subject 7 PNES

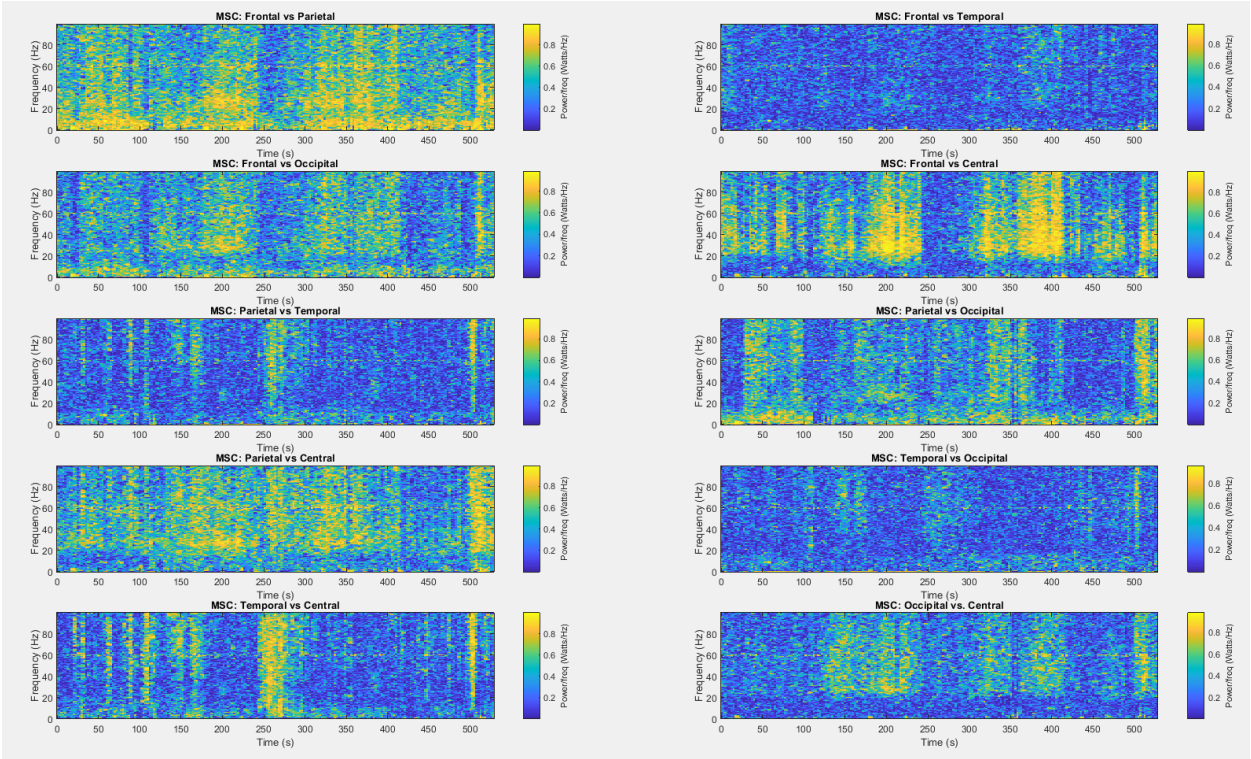

Figure B8. MSC Spectrograms between all region pairs: Subject 8 PNES

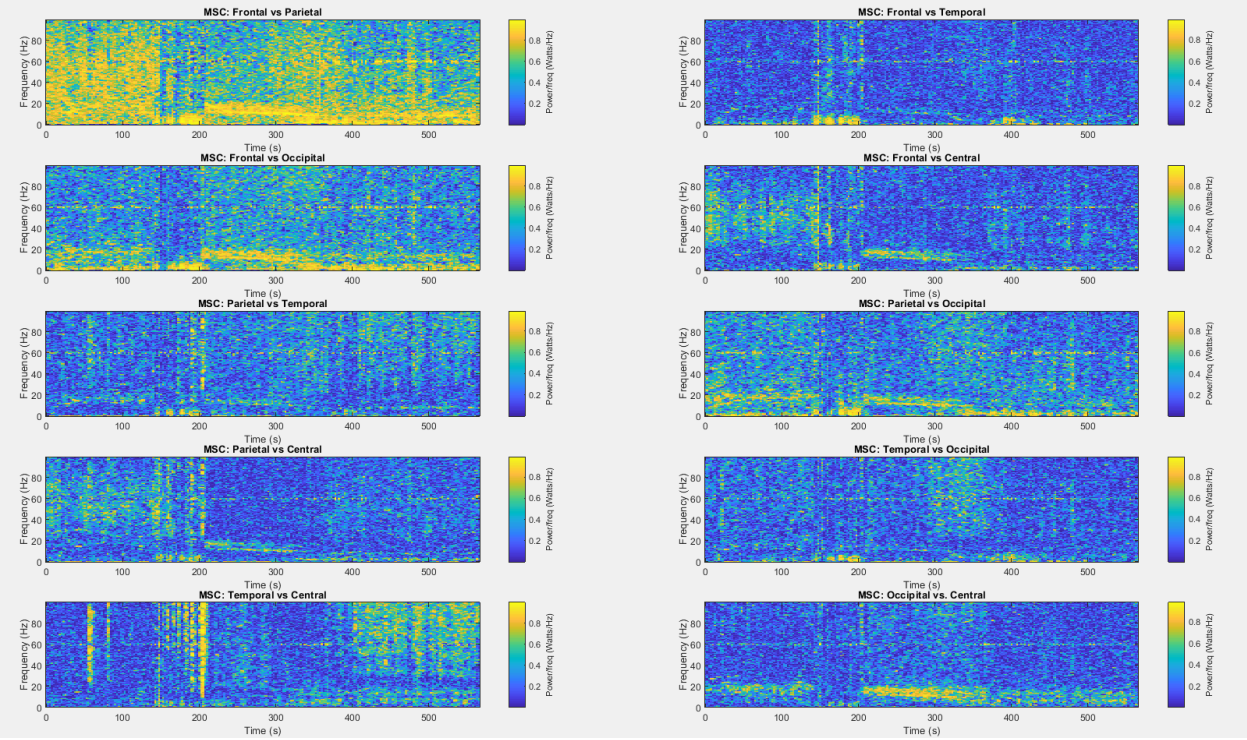

Figure B9. MSC Spectrograms between all region pairs: Subject 9 PNES

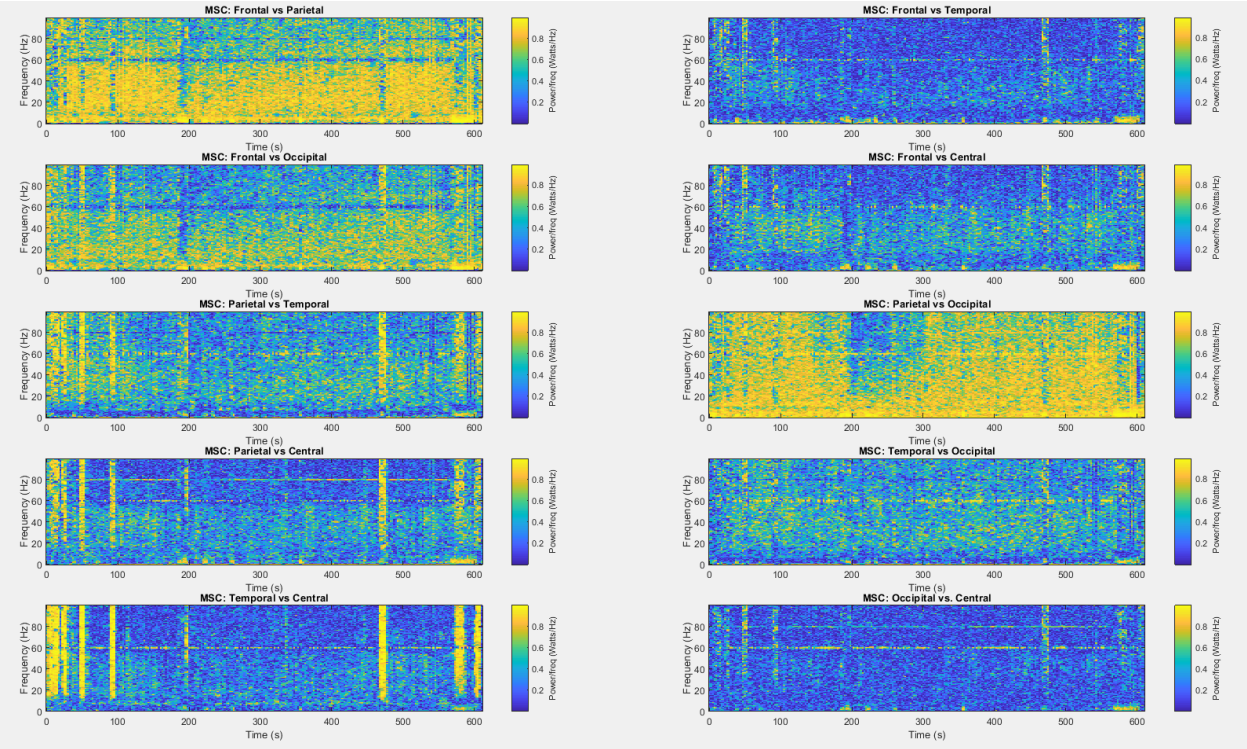

Figure B10. MSC Spectrograms between all region pairs: Subject 10 ES

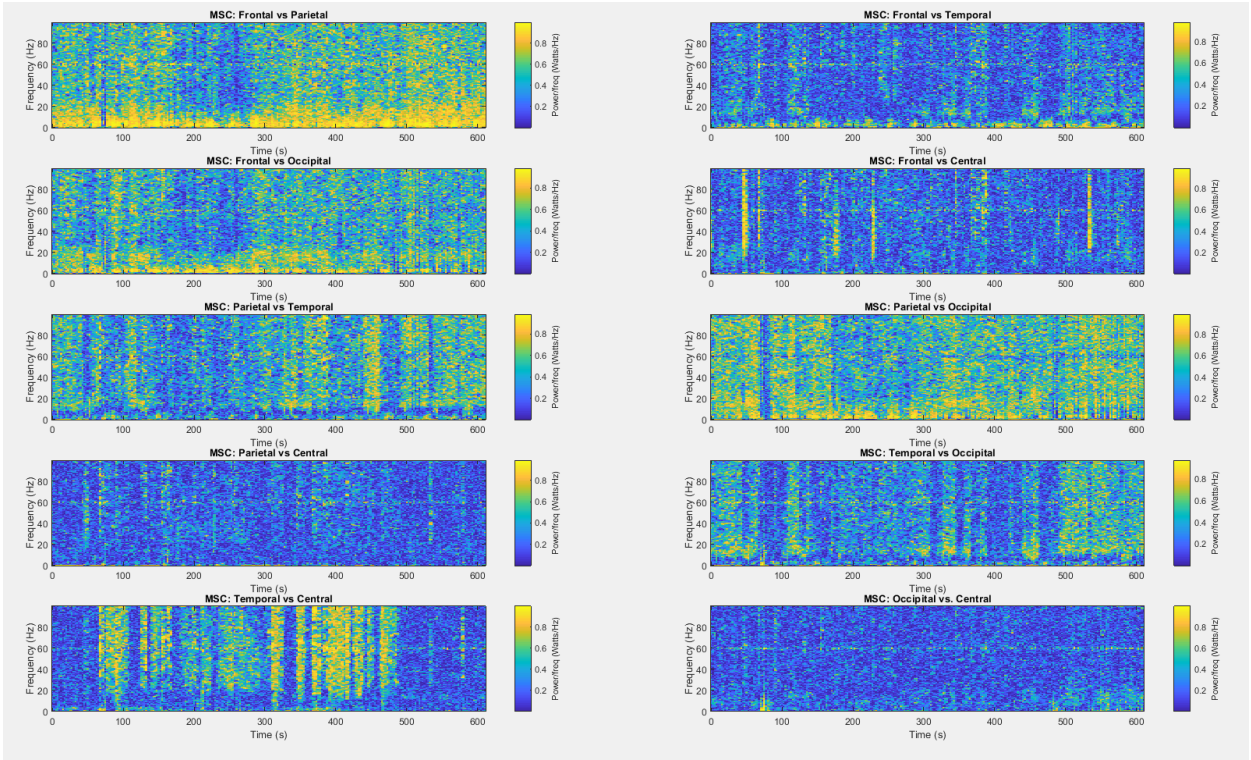

Figure B11. MSC Spectrograms between all region pairs: Subject 11 ES

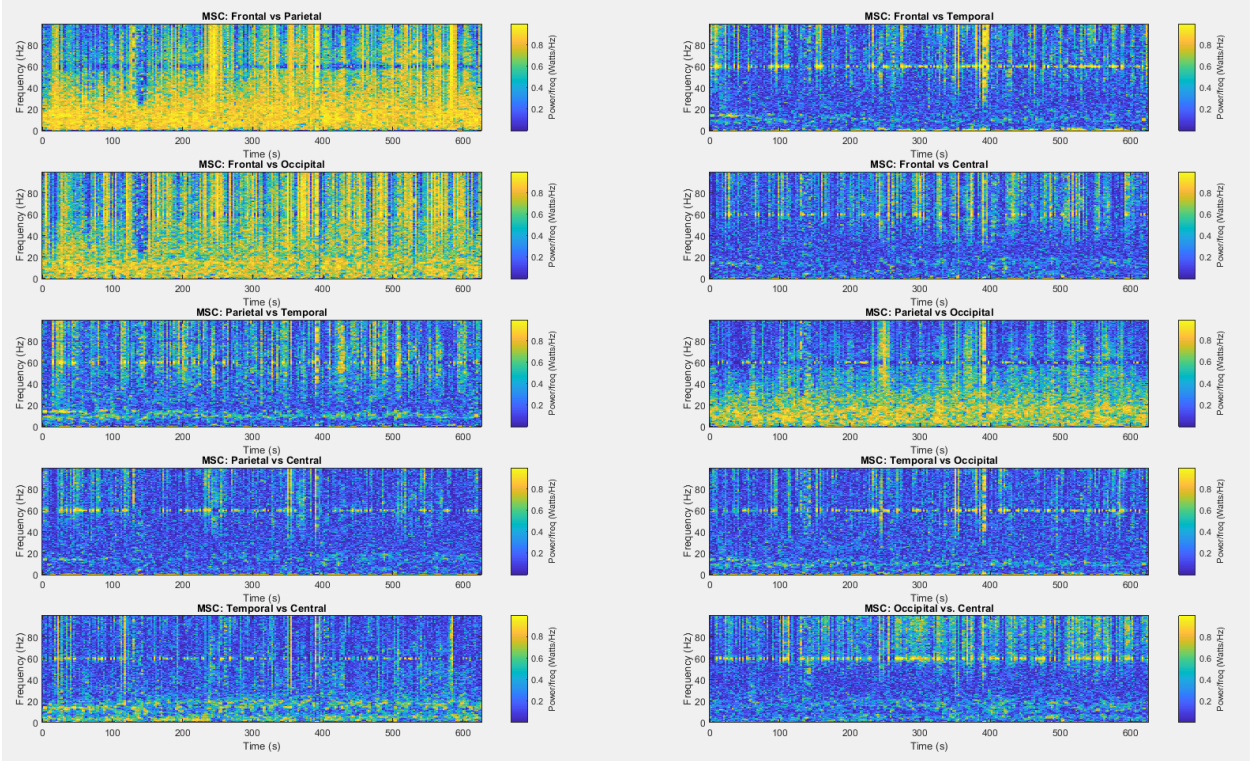

Figure B12. MSC Spectrograms between all region pairs: Subject 12 ES

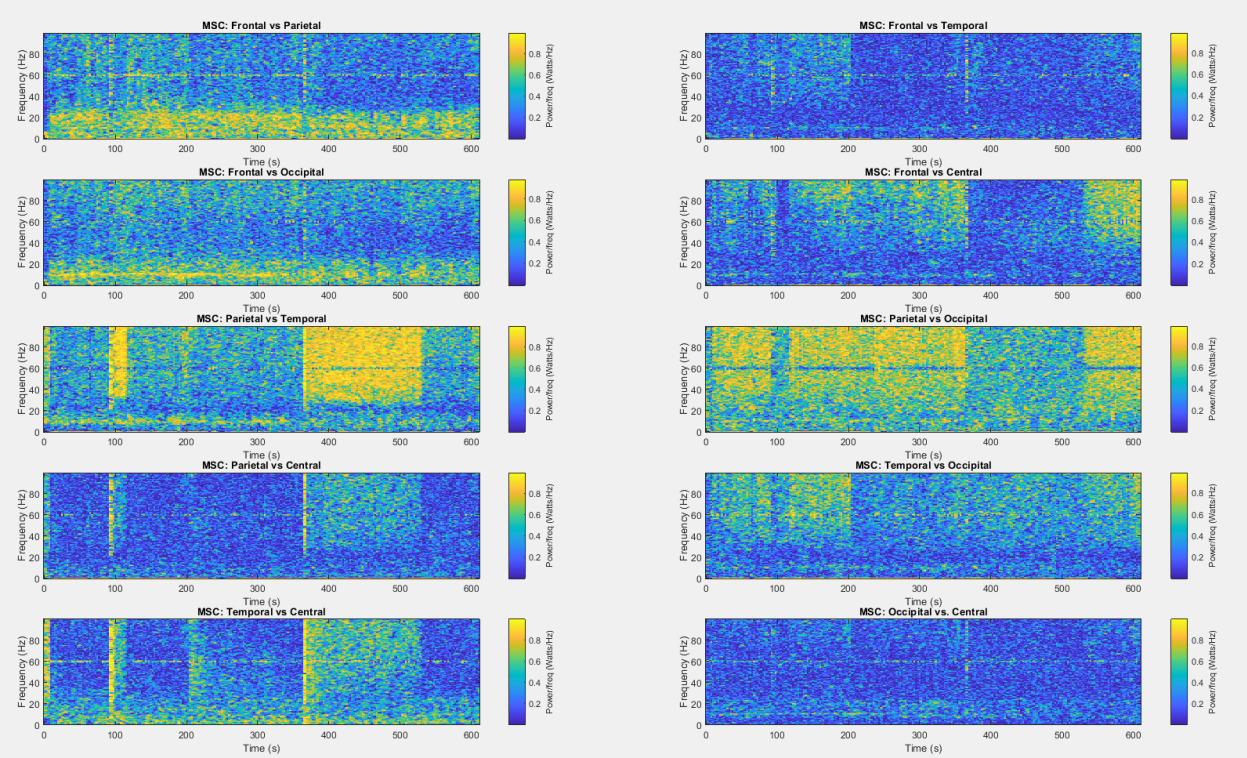

Figure B13. MSC Spectrograms between all region pairs: Subject 13 ES

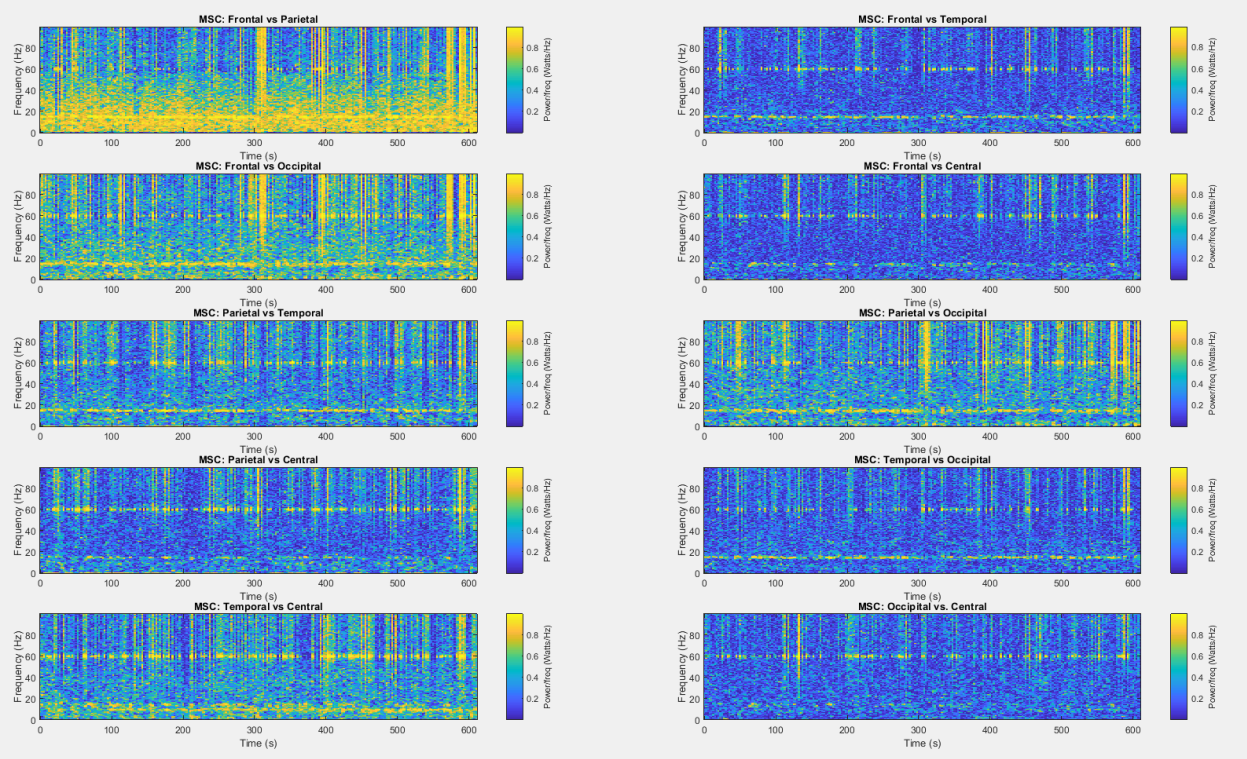

Figure B14. MSC Spectrograms between all region pairs: Subject 14 ES

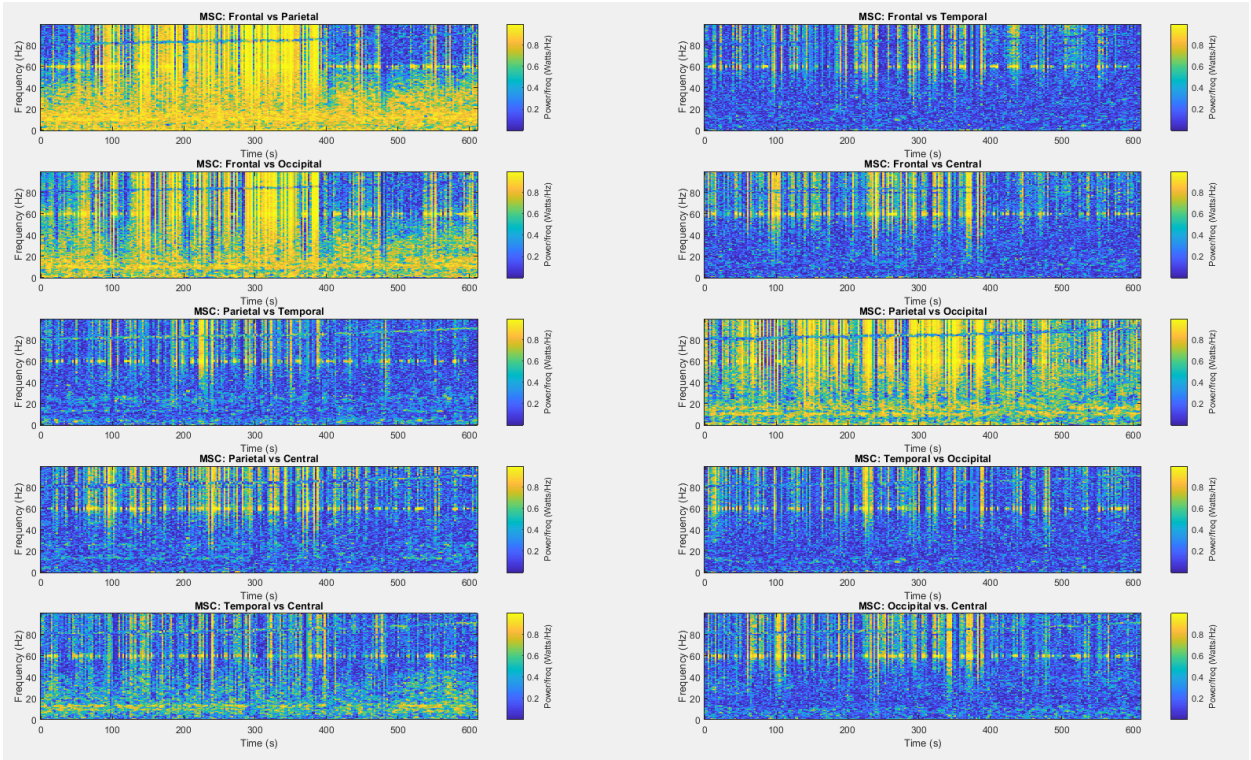

Figure B15. MSC Spectrograms between all region pairs: Subject 15 ES

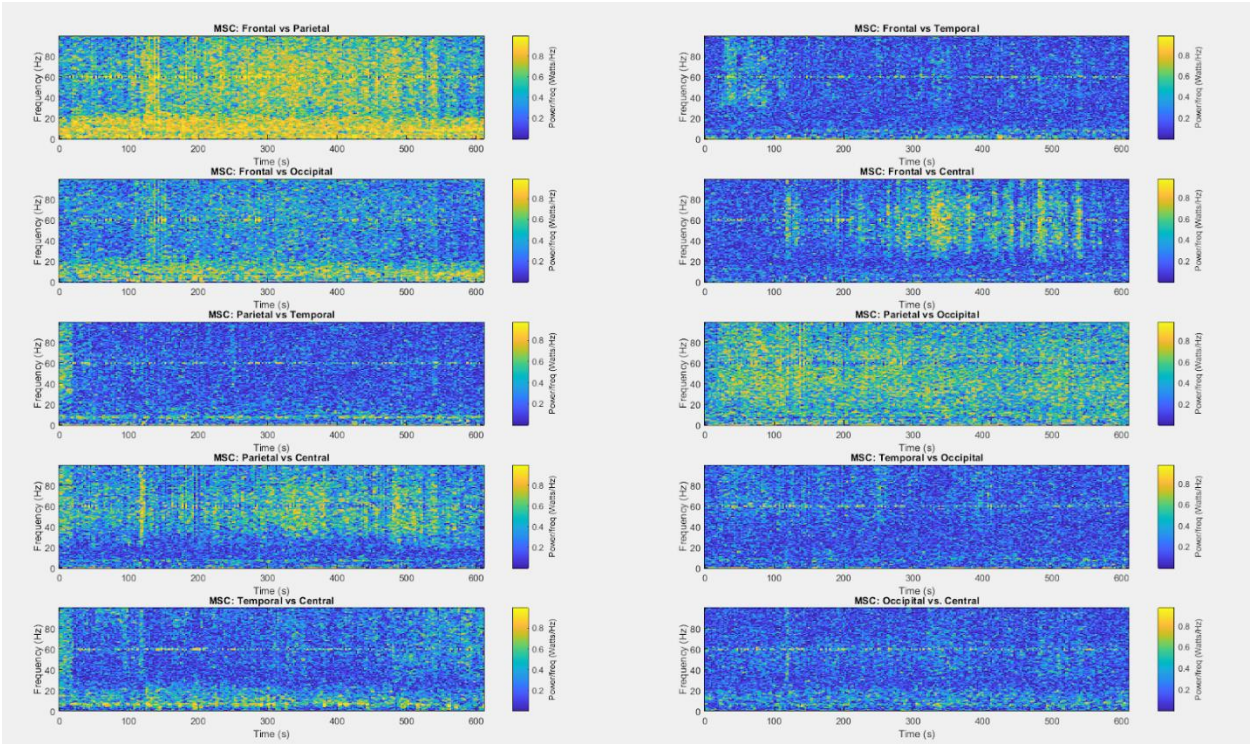

Figure B16. MSC Spectrograms between all region pairs: Subject 16 ES

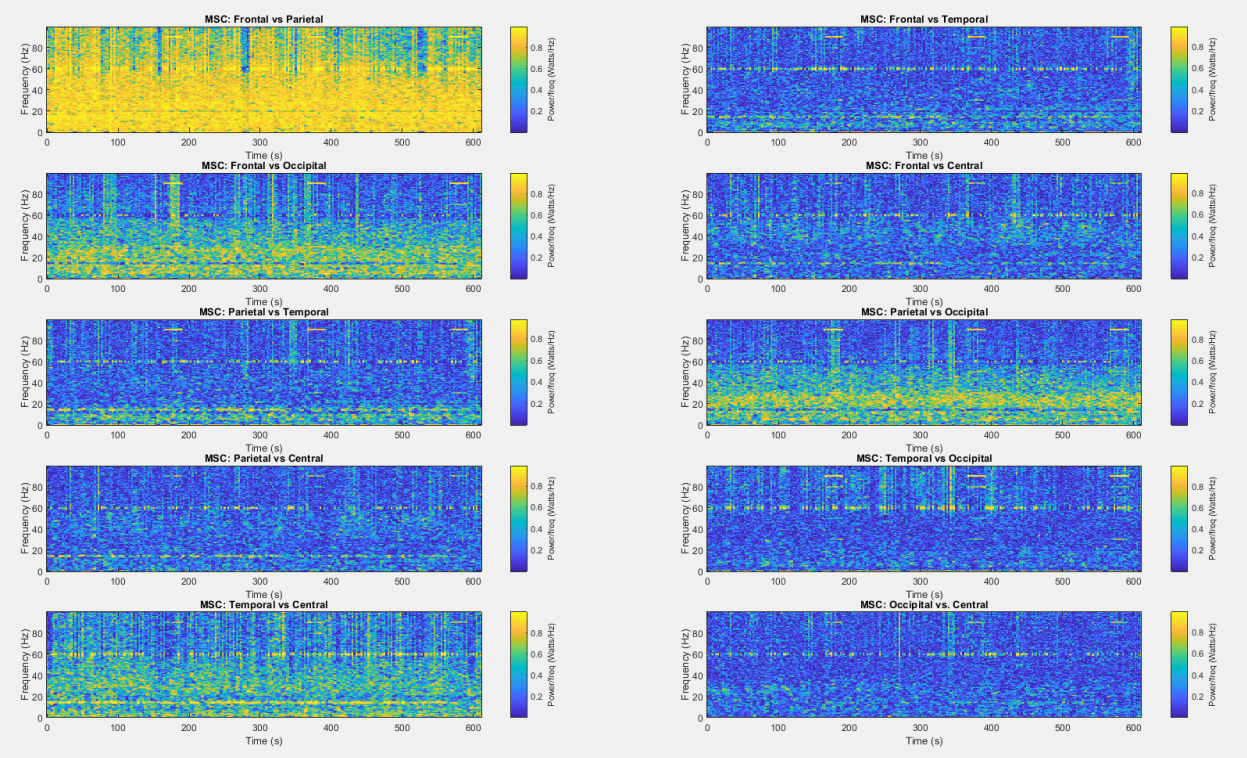

Figure B17. MSC Spectrograms between all region pairs: Subject 17 ES

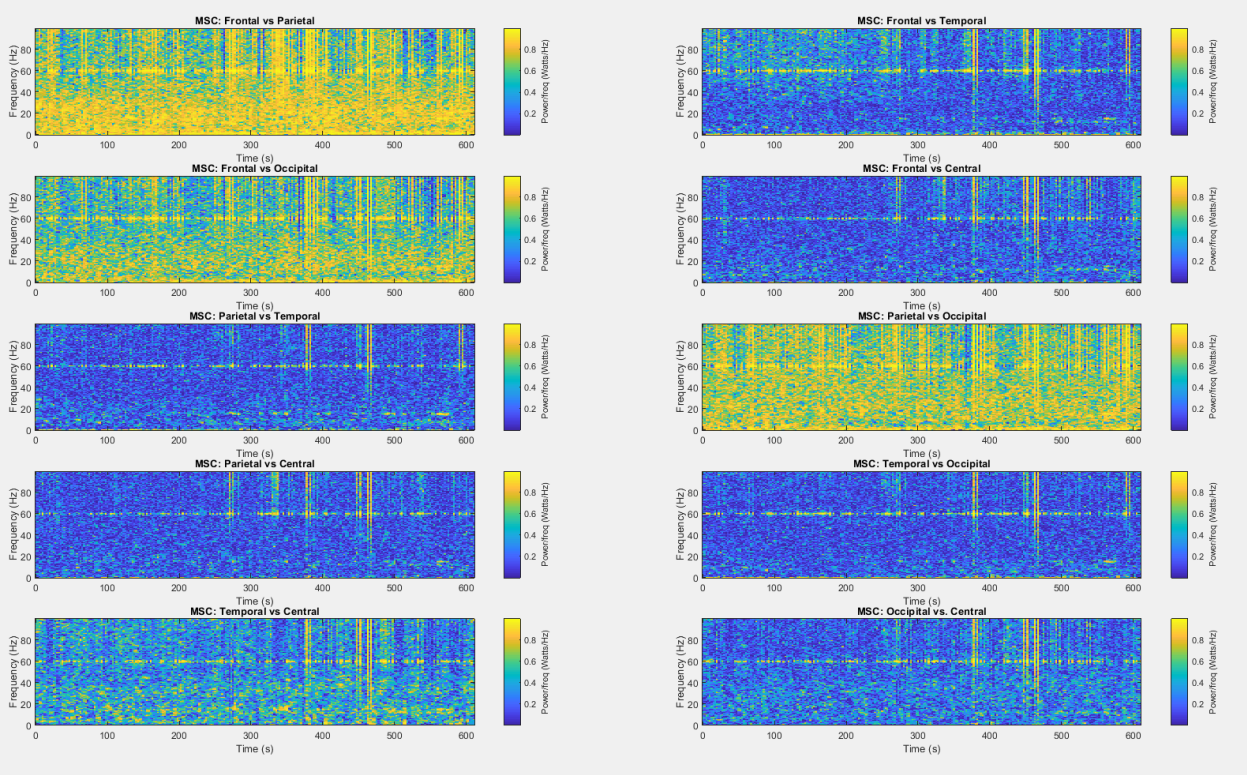

Figure B18. MSC Spectrograms between all region pairs: Subject 18 ES

Appendix C. Normality and Outliers

C.1 Normality

Table C.1.1. Results of the Shapiro-Wilk Test for normality of MSC in the Delta Band

Delta Band: Tests of Normality				
		Shapiro-Wilk		
PNES or ES		Statistic	Df	Sig.
MSC_FP	PNES	0.902	9	0.263
	ES	0.855	9	0.085
MSC_FT	PNES	0.842	9	0.061
	ES	0.910	9	0.318
MSC_FO	PNES	0.859	9	0.093
	ES	0.867	9	0.114
MSC_FC	PNES	0.859	9	0.092
	ES	0.678	9	0.001
MSC_PT	PNES	0.728	9	0.003
	ES	0.962	9	0.817
MSC_PO	PNES	0.971	9	0.900
	ES	0.873	9	0.133
MSC_PC	PNES	0.892	9	0.209
	ES	0.848	9	0.070
MSC_TO	PNES	0.902	9	0.263
	ES	0.919	9	0.388
MSC_TC	PNES	0.858	9	0.092
	ES	0.908	9	0.300
MSC_OC	PNES	0.870	9	0.123
	ES	0.955	9	0.746

Table C.1.2. Results of the Shapiro-Wilk Test for normality of MSC in the Theta Band

Theta Band: Tests of Normality				
		Shapiro-Wilk		
PNES or ES		Statistic	df	Sig.
MSC_FP	PNES	0.800	9	0.021
	ES	0.906	9	0.289
MSC_FT	PNES	0.852	9	0.078
	ES	0.907	9	0.298
MSC_FO	PNES	0.951	9	0.698
	ES	0.952	9	0.709
MSC_FC	PNES	0.874	9	0.135
	ES	0.886	9	0.183
MSC_PT	PNES	0.946	9	0.646
	ES	0.812	9	0.028
MSC_PO	PNES	0.949	9	0.682
	ES	0.950	9	0.695
MSC_PC	PNES	0.856	9	0.088
	ES	0.927	9	0.453
MSC_TO	PNES	0.955	9	0.750
	ES	0.808	9	0.025
MSC_TC	PNES	0.823	9	0.037
	ES	0.786	9	0.014
MSC_OC	PNES	0.954	9	0.738
	ES	0.956	9	0.752

Table C.1.3. Results of the Shapiro-Wilk Test for normality of MSC in the Alpha Band

Alpha Band: Tests of Normality				
		Shapiro-Wilk		
PNES or ES		Statistic	df	Sig.
MSC_FP	PNES	0.905	9	0.279
	ES	0.948	9	0.663
MSC_FT	PNES	0.864	9	0.106
	ES	0.964	9	0.837
MSC_FO	PNES	0.961	9	0.813
	ES	0.977	9	0.947
MSC_FC	PNES	0.941	9	0.594
	ES	0.943	9	0.619
MSC_PT	PNES	0.919	9	0.385
	ES	0.948	9	0.664
MSC_PO	PNES	0.912	9	0.330
	ES	0.965	9	0.845
MSC_PC	PNES	0.954	9	0.730
	ES	0.850	9	0.074
MSC_TO	PNES	0.872	9	0.130
	ES	0.902	9	0.263
MSC_TC	PNES	0.846	9	0.067
	ES	0.950	9	0.692
MSC_OC	PNES	0.961	9	0.804
	ES	0.931	9	0.492

Table C.1.4. Results of the Shapiro-Wilk Test for normality of MSC in the Beta Band

Beta Band: Tests of Normality				
		Shapiro-Wilk		
PNES or ES		Statistic	df	Sig.
MSC_FP	PNES	0.975	9	0.936
	ES	0.883	9	0.168
MSC_FT	PNES	0.922	9	0.406
	ES	0.851	9	0.077
MSC_FO	PNES	0.828	9	0.043
	ES	0.880	9	0.158
MSC_FC	PNES	0.708	9	0.002
	ES	0.694	9	0.001
MSC_PT	PNES	0.862	9	0.100
	ES	0.899	9	0.245
MSC_PO	PNES	0.955	9	0.749
	ES	0.962	9	0.821
MSC_PC	PNES	0.783	9	0.013
	ES	0.705	9	0.002
MSC_TO	PNES	0.853	9	0.081
	ES	0.795	9	0.018
MSC_TC	PNES	0.839	9	0.056
	ES	0.962	9	0.821
MSC_OC	PNES	0.932	9	0.497
	ES	0.923	9	0.420

Table C.1.5. Results of the Shapiro-Wilk Test for normality of MSC in the Gamma Band

Gamma Band: Tests of Normality				
		Shapiro-Wilk		
PNES or ES		Statistic	df	Sig.
MSC_FP	PNES	0.767	9	0.008
	ES	0.947	9	0.658
MSC_FT	PNES	0.967	9	0.868
	ES	0.908	9	0.301
MSC_FO	PNES	0.979	9	0.961
	ES	0.914	9	0.344
MSC_FC	PNES	0.837	9	0.053
	ES	0.918	9	0.377
MSC_PT	PNES	0.871	9	0.125
	ES	0.930	9	0.479
MSC_PO	PNES	0.947	9	0.660
	ES	0.901	9	0.259
MSC_PC	PNES	0.886	9	0.180
	ES	0.899	9	0.244
MSC_TO	PNES	0.782	9	0.013
	ES	0.852	9	0.079
MSC_TC	PNES	0.958	9	0.775
	ES	0.882	9	0.166
MSC_OC	PNES	0.941	9	0.590
	ES	0.870	9	0.124

Table C.1.6. Results of the Shapiro-Wilk Test for normality of C-ApEn

C-ApEn: Tests of Normality									
Group		Shapiro-Wilk			Group		Shapiro-Wilk		
		Statistic	Df	Sig.			Statistic	Df	Sig.
FP	PNES	0.702	9	0.001	PO	PNES	0.807	9	0.024
	ES	0.922	9	0.411		ES	0.971	9	0.905
PF	PNES	0.777	9	0.011	OP	PNES	0.770	9	0.009
	ES	0.963	9	0.831		ES	0.978	9	0.953
FT	PNES	0.740	9	0.004	PC	PNES	0.815	9	0.031
	ES	0.901	9	0.257		ES	0.946	9	0.643
TF	PNES	0.855	9	0.085	CP	PNES	0.865	9	0.107
	ES	0.903	9	0.270		ES	0.924	9	0.426
FO	PNES	0.733	9	0.003	TO	PNES	0.853	9	0.080
	ES	0.976	9	0.941		ES	0.942	9	0.605
OF	PNES	0.798	9	0.019	OT	PNES	0.795	9	0.018
	ES	0.970	9	0.892		ES	0.957	9	0.763
FC	PNES	0.766	9	0.008	TC	PNES	0.867	9	0.115
	ES	0.922	9	0.413		ES	0.890	9	0.200
CF	PNES	0.874	9	0.137	CT	PNES	0.864	9	0.105
	ES	0.969	9	0.889		ES	0.924	9	0.423
PT	PNES	0.790	9	0.016	OC	PNES	0.778	9	0.011
	ES	0.938	9	0.560		ES	0.971	9	0.907
TP	PNES	0.833	9	0.049	CO	PNES	0.810	9	0.026
	ES	0.900	9	0.250		ES	0.916	9	0.363

Table C.1.7. Results of the Shapiro-Wilk Test for normality of C-ApEn: Subjects 8 and 13 removed

C-ApEn: Tests of Normality (Subjects 8 and 13 removed)									
Group		Shapiro-Wilk			Group		Shapiro-Wilk		
		Statistic	Df	Sig.			Statistic	Df	Sig.
FP	PNES	0.950	8	0.710	PO	PNES	0.823	8	0.051
	ES	0.945	8	0.661		ES	0.975	8	0.932
PF	PNES	0.918	8	0.414	OP	PNES	0.719	8	0.004
	ES	0.962	8	0.824		ES	0.961	8	0.820
FT	PNES	0.908	8	0.339	PC	PNES	0.893	8	0.251
	ES	0.916	8	0.398		ES	0.936	8	0.575
TF	PNES	0.899	8	0.283	CP	PNES	0.846	8	0.087
	ES	0.884	8	0.205		ES	0.950	8	0.712
FO	PNES	0.803	8	0.031	TO	PNES	0.827	8	0.055
	ES	0.980	8	0.961		ES	0.928	8	0.495
OF	PNES	0.757	8	0.010	OT	PNES	0.796	8	0.026
	ES	0.965	8	0.852		ES	0.980	8	0.963
FC	PNES	0.947	8	0.684	TC	PNES	0.886	8	0.214
	ES	0.921	8	0.439		ES	0.880	8	0.188
CF	PNES	0.859	8	0.118	CT	PNES	0.843	8	0.081
	ES	0.984	8	0.981		ES	0.944	8	0.646
PT	PNES	0.881	8	0.191	OC	PNES	0.771	8	0.014
	ES	0.929	8	0.508		ES	0.984	8	0.981
TP	PNES	0.858	8	0.114	CO	PNES	0.762	8	0.011
	ES	0.884	8	0.207		ES	0.904	8	0.314

C.2 Outliers

Table C.2.1. Presence of outliers for MSC results

MSC: Outliers by Subject Number						
Group		Delta MSC	Theta MSC	Alpha MSC	Beta MSC	Gamma MSC
FP	PNES	1	1	x	x	4
	ES	13	13	x	x	X
FT	PNES	4	4	4	x	X
	ES	X	X	x	x	X
FO	PNES	X	X	x	x	X
	ES	X	X	14,15	x	X
FC	PNES	4	X	x	8	8
	ES	10	10	x	10	X
PT	PNES	4	X	x	x	X
	ES	X	X	13,15	x	X
PO	PNES	X	9	2,5,8,9	x	X
	ES	X	X	x	x	X
PC	PNES	X	X	x	8	X
	ES	10	X	10	10	X
TO	PNES	4	7	x	6	X
	ES	X	15	x	x	X
TC	PNES	X	X	2	x	X
	ES	X	10,11	11,14	x	X
CO	PNES	X	X	x	x	X
	ES	X	X	x	18	X

Table C.2.2. Presence of outliers for C-ApEN results

Cross Approximate Entropy					
Group		Outliers by Subject Number	Group		Outliers by Subject Number
FP	PNES	8	PO	PNES	X
	ES	X		ES	X
PF	PNES	8	OP	PNES	X
	ES	X		ES	X
FT	PNES	8	PC	PNES	8
	ES	X		ES	X
TF	PNES	8	CP	PNES	X
	ES	X		ES	X
FO	PNES	8	TO	PNES	X
	ES	X		ES	X
OF	PNES	X	OT	PNES	X
	ES	13		ES	13
FC	PNES	8	TC	PNES	X
	ES	X		ES	X
CF	PNES	X	CT	PNES	X
	ES	X		ES	X
PT	PNES	8	OC	PNES	X
	ES	X		ES	X
TP	PNES	X	CO	PNES	X
	ES	X		ES	13,15,16

Table C.2.3. Presence of outliers for C-ApEN results: Subjects 8 and 13 removed

Cross Approximate Entropy					
Group		Outliers by Subject Number	Group		Outliers by Subject Number
FP	PNES	X	PO	PNES	X
	ES	X		ES	X
PF	PNES	X	OP	PNES	X
	ES	X		ES	X
FT	PNES	X	PC	PNES	X
	ES	X		ES	X
TF	PNES	X	CP	PNES	X
	ES	X		ES	X
FO	PNES	X	TO	PNES	X
	ES	X		ES	X
OF	PNES	X	OT	PNES	X
	ES	X		ES	X
FC	PNES	X	TC	PNES	X
	ES	X		ES	X
CF	PNES	X	CT	PNES	X
	ES	X		ES	X
PT	PNES	X	OC	PNES	X
	ES	X		ES	X
TP	PNES	X	CO	PNES	X
	ES	X		ES	15,16

Appendix D. MATLAB Code

Preprocessing and plotting of MSC results

```
%%%%%%%%%%%%%%%%%%%%%%%%%%%%%%%%%%%%%%%%%%%%%%%%%%%%%%%%%%%%%%%%%%%%%%%%%%%%
% Title: MSC_lobes.m
% Author: Sarah Barnes
% Description: Imports subject EEG data, handles preprocessing, averages
% signals into lobe regions, gets MSC between regions for each
% subject, and plots MSC results.
%%%%%%%%%%%%%%%%%%%%%%%%%%%%%%%%%%%%%%%%%%%%%%%%%%%%%%%%%%%%%%%%%%%%%%%%%%%%

%% Importing subject EEG data
% Array to store path for each subject's EEG data
subjectPath = [<paths for subject data here>]

% Array to store subject number strings
subjectNum = [<Subject numbers, e.g. "Subject 1">];

% storing all subject data
for i = 1:length(subjectPath)
    data = load(subjectPath(i));
    EEG.Subject(i) = data;
    data.Data = [];
end

%% Preallocation for each region pair field
subject = struct('FP', cell(1, 18), 'FT', cell(1, 18),...
 'FO', cell(1,18), 'FC', cell(1,18), 'PT', cell(1,18),...
 'PO', cell(1,18), 'PC', cell(1,18), 'TO', cell(1,18),...
 'TC', cell(1,18), 'OC', cell(1,18));

% This for loop iterates through each subject, pulls in the EEG data and
% calculates MSC
for s = 1:length(SubjectNum)
    clear n;
    EEG_data = [];
    EEG_data = [EEG.Subject(s).Data];


    %% Signal preprocessing
    % 60 Hz notch filter to remove mains interference
    d = designfilt('bandstopiir','FilterOrder',2, ...
               'HalfPowerFrequency1',59,'HalfPowerFrequency2',61, ...
               'DesignMethod','butter','SampleRate',200);

    % Application of notch filter to EEG signals
    EEG_data = filtfilt(d,EEG_data);

    % Application of reference average
    EEG_data = EEG_data';
    EEG_data = (EEG_data-mean(EEG_data));
```

```
    % Channel info and sampling frequency
    load('Channels.mat'); load('Fs.mat');

    %% Channel averaging to obtain on time series representing each region
    % Frontal Region is shown for example, repeat for all regions
    % Frontal lobe channels: Channel 1 = Fp1, Channel 2 = Fp2,
    % Channel 3 = F3, Channel 4 = Fp4, Channel 11 = F7, Channel 12 = F8

    frontal = EEG_data([1,2,3,4,11,12],:);

    % Average of frontal lobe EEG signals
    avgF = mean(frontal);

    %% Parameters
    Fs = 200; % Sampling frequency of EEG signals
    nfft = 1200; % number of points for fft
    M = 1200; % Window Length (6 second window)
    L = 7; % Number of unique windows
    H = 3.5; % Time half bandwidth
    timeInc = 600; % Time increment (50% overlap)
    f = 0:Fs/nfft:Fs/2-Fs/nfft; % frequency vector
    n = (1:timeInc:length(EEG_data)-M)/Fs; % Time axis

    %% Window creation using DPSS()
    [dps, lambda] = dpss(M,H,L); % window length by window number 1000 X 7
    dps = dps'; % 7 by 1000 (invert)

    %% Getting MSC between each region pair.
    % Frontal vs Parietal is shown as an example, repeat this step for
    % each region pair of interest
    % Calling the short term eigen transform function
    X = steigen(avgF, dps, L, timeInc, nfft); % Frontal data
    Y = steigen(avgP, dps, L, timeInc, nfft); % Parietal data

    % Calculating MSC
    FP_MSC = MSC(X,Y)'; % MSC between frontal and parietal

    % Storing MSC results
    subject(s).FP = FP_MSC(1:nfft/2, :);

    % Plotting MSC Spectrograms
    figure
    set(gcf,'name',SubjectName(s),'numbertitle','off')
    subplot(5,2,1)
    imagesc(n, f, (FP_MSC(1:nfft/2, :))); view(0,-90);
    xlabel('Time Segment (6s)'); ylabel('Frequency (Hz)');
    title('MSC: Frontal vs Parietal');
    b = colorbar; % colorbar to show power/freq
    ylabel(b, 'Power/freq (Watts/Hz)');

   clear temporal; clear parietal; clear occipital; clear frontal;
   clear central;
   X = []; Y = [];
End
```

Short Term Minimum Bias Eigen Transform

```
%%%%%%%%%%%%%%%%%%%%%%%%%%%%%%%%%%%%%%%%%%%%%%%%%%%%%%%%%%%%%%%%%%%%%%%%%%%%%%%
% Title: steigen.m
% Author: Sarah Barnes
% Description: Computes short term minimum bias transform of input data x
% See details below
%%%%%%%%%%%%%%%%%%%%%%%%%%%%%%%%%%%%%%%%%%%%%%%%%%%%%%%%%%%%%%%%%%%%%%%%%%%%%%%

function [transform] = steigen(x, V, L, ti, nfft)
% [transform] = steigen(x, V, L, ti, nfft)
%
% This function will return an array containing the short term
%   minimum bias eigen transform
%
% Inputs to the function
% x: The input data vector
% V: Array containing L windows
% L = Number of window sequences
% ti: Time increment: Evaluate X[n,k] at ti
% nfft: Number of fft points
%
% Outputs to the function
%  coherence: short term minimum bias eigen transform
%
% AUTHOR: S. Barnes
% DATE: 11/21/2018

% Input Argument Error check
if(nargin < 1)
    fprintf(1,'Please provide data. Type help steigen\n');
    return;
end

M = length(V); % window length
N = length(x); % length of input data vector

% Preallocation for X array
X = zeros(length((M/2):ti:(N-M/2)) , nfft , L);

% Computing the short term eigen trasform
for l = 1:L % Step through each window sequence
    i =0;
    temp = zeros(length((M/2):ti:(N-M/2)) , nfft);
    for m = (M/2):ti:(N-M/2)
        i=i+1;
        % Take fft of x*V
        temp(i,:) = fft( x((m+1-M/2):(m+M/2)).*V(l, 1:M) ,nfft);
    end
    X(:,:,l) = temp; % Store X by window sequence
end

transform = X; % Store X in output
```

Magnitude Squared Coherence Calculation

```
%%%%%%%%%%%%%%%%%%%%%%%%%%%%%%%%%%%%%%%%%%%%%%%%%%%%%%%%%%%%%%%%%%%%%%%%%%%%%%%
% Title: MSC.m
% Author: Sarah Barnes
% Description: Computes the magnitude squared coherence between two data
% vectors. See details below
%%%%%%%%%%%%%%%%%%%%%%%%%%%%%%%%%%%%%%%%%%%%%%%%%%%%%%%%%%%%%%%%%%%%%%%%%%%%%%%

function [coherence, SXX, SYY, SXY] = MSC(X, Y)
%  [coherence] = MSC(x, y)
%
% This function will return the Magnitude-Squared Coherence from two input
% sets of data
%
% Inputs to the function
% x: The first input data vector
% y: The second input data vector
%
% Outputs to the function
%  coherence: Magnitude Squared Coherence
%  SXX: Power Spectrum of X
%  SYY: Power Spectrum of Y
%  SXY: Cross Power Spectrum of X and Y
%
% AUTHOR: S. Barnes
% DATE: 11/21/2018

% Input Argument Error check
if(nargin < 1)
    fprintf(1,'Please provide data. Type help MSC\n');
    return;
end

% Power Spectrums and MSC
SXX = sum(abs(X).^2,3);
SYY = sum(abs(Y).^2,3);
SXY = abs(sum( (X.*conj(Y)) ,3)).^2;
coherence = SXY./(SXX.*SYY);
```

Cross Approximate Entropy

* Refer to MSC preprocessing section for details on importing subject data and preprocessing (D.1)

```
%%%%%%%%%%%%%%%%%%%%%%%%%%%%%%%%%%%%%%%%%%%%%%%%%%%%%%%%%%%%%%%%%%%%%%%%%%%%%%%
% Title: CApEn.m
% Author: Sarah Barnes
% Description: Computes the cross approximate entropy of two time series.
% See details below.
%%%%%%%%%%%%%%%%%%%%%%%%%%%%%%%%%%%%%%%%%%%%%%%%%%%%%%%%%%%%%%%%%%%%%%%%%%%%%%%

function[crossApproximateEntropy]=xApEntropy(X,Y)
% [crossApproximateEntropy] = xApEntropy(X,Y)
%
% This function will return the cross approximate entropy of two time
% series x and y.
```

```
%
% Inputs to the function
% x,y: Input time series data, normalized (sd=1)
%
% Outputs to the function
% crossApproximateEntropy: Cross approximate entropy for x and y
%
% AUTHOR: S. Barnes
% DATE: 09/01/2019

% Parameters
N=length(X); % The length of the time series, x and y should be of the same
length
r = 0.2; % This is the threshold filter, typically 0.2*sd, since the data
         % are normalized, it is just 0.2
M = 2; % The embedded dimension

for m = M:M+1 % evaluate at m = 2 and m = 3, to compare occurence of m
              % point patterns to m+1 point patterns
    C = zeros(1,N);

    for i=1:(N-m+1)
        x = X(i:i+m-1);
        Nxy = 0;
        for j=1:(N-m+1)
            y = Y(j:j+m-1);
            dif=(abs(x-y)<=r);
            count = all(dif);
            Nxy = Nxy + count;
        end
        C(i) = Nxy / (N-m+1);
    end
    logC = log(C);
    logC(isinf(logC)) = [];
    phi(m) = mean(logC);
end
crossApproximateEntropy = phi(2) - phi(3);
```

Bibliography

[1] R. S. Fisher et al., "Epileptic Seizures and Epilepsy: Definitions Proposed by the International League Against Epilepsy (ILAE) and the International Bureau for Epilepsy (IBE)," *Epilepsia,* vol. 46, no. 4, p. 470-472, 2005.

[2] O. Devinsky, D. Gazzola and W. C. LaFrance Jr, "Differentiating between nonepileptic and epileptic seizures," *Nature Reviews Neurology,* vol. 7. P 210-220, 2011.

[3] R. J. Brown et al., "Psychogenic nonepileptic seizures," *Epilepsy and Behavior,* vol. 22, p.85-93, 2011.

[4] P. Xu et al., "Differentiating Between Psychogenic Nonepileptic Seizures and Epilepsy Based on Common Spatial Pattern of Weighted EEG Resting Networks," *IEEE Transactions on Biomedical Engineering,* vol. 61, no. 6, p. 1747-1755, 2014.

[5] N. M. G. Bodde et al., "Psychogenic non-epileptic seizures—Diagnostic issues: A critical review," *Clinical Neurology and Neurosurgery,* vol. 111, p. 1-9, 2009.

[6] Z. Mei, X. Zhaa, H. Chen, and W. Chen, "Bio-Signal Complexity Analysis in Epileptic Seizure Monitoring: A Topic Review," *Sensors,* vol. 18, p. 1720-1747, 2018.

[7] G. Wang et al., "Epileptic Seizure Detection Based on Partial Directed Coherence Analysis," *IEEE Journal of Biomedical and Health Informatics,* vol. 20, no. 3, p. 873-879, 2016.

[8] U. R. Acharya et al., "Application of entropies for automated diagnosis of epilepsy using EEG signals: A review," *Knowledge Based Systems,* vol. 88, p. 85-96, 2015.

[9] N. Kannathal, M. L. Choo, U. R. Acharya, and P. K. Sadasivan, "Entropies for detection of epilepsy in EEG," *Computer Methods and Programs in Biomedicine,* vol. 80, p. 187-194, 2005.

[10] D. P. Subha, P. K. Joseph, R. Acharya, and C. M. Lim, "EEG Signal Analysis: A Survey," *Journal of Medical Systems,* vol. 34, p. 195-212, 2010.

[11] D. Gajic, Z. Djurovic, J. Gligorijevic, S. DiGennaro, and I. Savic-Gajic, "Detection of epileptiform activity in EEG signals based on time-frequency and non-linear analysis," *Frontiers in Computational Neuroscience,* vol. 9, no. 38, p. 1-16, 2015.

[12] V. Sakkalis, "Review of advanced techniques for the estimation of brain connectivity measured with EEG/MEG," *Computers in Biology and Medicine,* vol. 41, p. 1110-1117, 2011.

[13] S. Tiran, P. Maurine, "SCA with Magnitude Squared Coherence," *Smart Card Research and Advanced Applications,* CARDIS 2012, Lecture Notes in Computer Science, vol. 7771, Springer, Berlin, Heidelberg, 2013.

[14] J. P. Noel et al., “Multisensory temporal function and EEG complexity in patients with epilepsy and psychogenic nonepileptic events”, *Epilepsy and Behavior,* vol. 70, p. 166-172, 2017.

[15] S. J. Ruiz-Gomez et al., “Measuring Alterations of Spontaneous EEG Neural Coupling in Alzheimer's Disease and Mild Cognitive Impairment by Means of Cross-Entropy Metrics,” *Frontiers in Neuroinformatics,* vol. 12, p. 76-86, 2018.

[16] J. Licinio et al., “Synchronicity of frequently sampled, 24-h concentrations of circulating leptin, luteinizing hormone, and estradiol in healthy women,” *Proceedings of the National Academy of Sciences of the United States of America,* vol. 95, no. 5, p. 2541-2546, 1998.

[17] J. J. Falco-Walters, I. E. Scheffers, & R. S. Fisher, “The new definition and classification of seizures and epilepsy”, *Epilepsy Research,* vol 139, p. 73-79, 2018.

[18] I. Manuel, and B. Núñez, 10-20 International System of Electrode Placement. Figure, (n.d).

[19] E. G. Lovett and K. M. Ropella, “Time-frequency coherence analysis of atrial fibrillation termination during procainamide administration,” *Annals of Biomedical Engineering,* vol. 25, no. 6, p. 975–984, 1997.

[20] S. Pincus, “Approximate entropy (ApEn) as a complexity measure,” *Chaos: An Interdisciplinary Journal of Nonlinear Science,* vol. 5, no. 1, p. 110–117, 1995.

[21] A H Mooij et al., “Differentiating epileptic from non-epileptic high frequency intracerebral EEG signals with measures of wavelet entropy”, *Clinical Neurophysiology,* vol. 127, p. 3529–3536, 2016.

[22] Q. Xue et al., “Altered brain connectivity in patients with psychogenic non-epileptic seizures: A scalp electroencephalography study”, *Journal of International Medical Research*, Vol. 41, No. 5, p.1682–1690, 2013.

[23] R. Li et al., “Altered regional activity and inter-regional functional connectivity in psychogenic non-epileptic seizures”, *Scientific Reports*, Vol. 5, No.1, 2015.

[24] S. Siuly, Y. Li, and Y. Zhang, “EEG Signal Analysis and Classification”, Switzerland: Springer, 2016.

[25] J. Zhang et al., “Pattern Classification of Large-Scale Functional Brain Networks: Identification of Informative Neuroimaging Markers for Epilepsy”, *PLoS ONE*, Vol. 7, No. 5, 2012.

[26] Y. Fusheng, H. Bo, and T. Qingyu, “Approximate Entropy and Its Application in Biosignal Analysis,” *Nonlinear Biomedical Signal Processing,* Piscataway, NJ, IEEE Press, vol. 2, p.72-90, 2001.

[27] D. J. Thurman et al., “Standards for epidemiologic studies and surveillance of epilepsy”, *Epilepsia,* vol. 52, p. 2–26, 2011.

[28] C. E. Elger & C. Hoppe, “Diagnostic challenges in epilepsy: seizure under-reporting and seizure detection”, *Lancet Neural,* vol. 17, p. 279-288, 2018.

[29] H. Patel et al., “Psychogenic Nonepileptic Seizures (Pseudoseizures)”, *Pediatrics in Review,* vol. 32, p. 66-72, 2011.

[30] R. J. Brown & M. Reuber, “Towards an integrative theory of psychogenic non-epileptic seizures (PNES)”, *Clinical Psychology Review,* vol. 47, p. 55-70, 2016.

[31] M. Herskovitz, “Stereotypy of Psychogenic Nonepileptic Seizures”, *Epilepsy and Behavior*, vol. 70, p. 140-144, 2017.

[32] D. Wasserman & M. Herskovitz, “Epileptic vs Psychogenic Nonepileptic Seizures: A Video-Based Survey”, *Epilepsy and Behavior,* vol. 73, p. 42-45, 2017.

[33] B. T. Tyson et al., “Differentiating epilepsy from psychogenic nonepileptic seizures using neuropsychological test data”, *Epilepsy and Behavior,* vol. 87, p. 39-45, 2018.

[34] M. Mcsweeney, M. Reubers, & L. Levita, “Neuroimaging studies in patients with psychogenic non-epileptic seizures: A systematic meta-review”, *Neuroimage: Clinical,* vol. 16, p. 210-221, 2017.

[35] J. W. Clark, M. R. Newman, W. H. Olson, and J. G. Webster, “Medical Instrumentation: Application and Design”, New York, NY: Wiley, 2010.

[36] M. J. Selesko, "Time Evolution of ECoG Network Connectivity in Patients with Refractory Epilepsy", *Masters Theses*. 897, 2018. https://scholarworks.gvsu.edu/theses/897

[37] A. G. Mahapatra, B. Singh, H. Wagatsuma, and K. Horio, “Epilepsy EEG Classification using Morphological Component Analysis”, *Journal on Advances in Signal Processing,* vol. 52, 2018.

[38] S. R. Benbadis and K. Lin, “Errors in EEG Interpretation and Misdiagnosis of Epilepsy”, *European Neurology,* vol. 59, p. 267-271, 2008.

[39] S. Burnos, P. Hilfiker, O. Sürücü, F. Scholkmann, N. Krayenbühl, T. Grunwald, and J. Sarnthein, “Human Intracranial High Frequency Oscillations (HFOs) Detected by Automatic Time-Frequency Analysis,” *PLoS ONE*, vol. 9, no. 4, 2014.

[40] D. Tuncel, A. Dizibuyuk, and M. K. Kiymik, “Time Frequency Based Coherence Analysis Between EEG and EMG Activities in Fatigue Duration,” *Journal of Medical Systems*, vol. 34, no. 2, pp. 131–138, 2008.

[41]] S. A. Taplidou and L. J. Hadjileontiadis, “Wheeze detection based on time-frequency analysis of breath sounds,” *Computers in Biology and Medicine*, vol. 37, no. 8, pp. 1073–1083, 2007.

[42] A. Goenka, A. Boro, and E. Yozawitz “Assessing quantitative EEG spectrograms to identify non-epileptic events,” *Epileptic Disord,* vol. 19, no. 3, p. 299-306, 2017.

[43] S. Pincus and W. Huang, “Approximate Entropy: Statistical Properties and Applications,” *Communications in Statistics – Theory and Methods,* vol. 21, no. 11, p 2061-3077, 1992.

[44] Z. Zhang et al., “Approximate entropy and support vector machines for electroencephalogram signal classification,” *Neural Regen Research,* vol. 8, no. 20, p. 1844-1852, 2013.

[45] M. Zarzuela et al., “Cross Approximate Entropy Parallel Computation on GPUs for Biomedical Signal Analysis. Application to MEG Recordings,” *Computer Methods and Programs in Biomedicine,* vol. 112, no. 1, p. 189-199, 2013.